LONG-TERM ATMOSPHERIC MEASUREMENT AND INTERPRETATION
(OF RADIATIVELY ACTIVE TRACE GASES)

DECC contract number: GA0201

Report (Nov 2014 - May 2015)

Date: 1st Jun 2015

University of Bristol: Simon O'Doherty, Aoife Grant, Kieran Stanley, Dan Say, Ann Stavert

Met Office: Alistair J. Manning, Tim Arnold

rdscientific: Richard G. Derwent

INSCON: Peter Simmonds

Terra Modus: Dickon Young

UEA: Stephen Humphrey, Bill Sturges, Sander van der Laan

1 Contents

1 Contents 2
2 Executive Summary 3
2.1 Project Summary 3
3 Overview of Progress 4
3.1 Update website 4
3.2 Investigating uncertainties in InTEM and the impact of using the different stations 5
3.3 Direction specific baselines developed within InTEM 5
3.4 NF_3 emissions across East Asia 5
3.5 RAC model analysis 5
4 Update on UK DECC network measurement sites 6
4.1 Mace Head (MHD) 6
4.2 Tacolneston (TAC) 6
4.3 Ridge Hill (RGL) 6
4.4 Angus (TTA) 6
6 Assessing the Impact of the different stations in the UK DECC network 7
6.1 Introduction 7
6.2 Method 7
6.3 Summary 14
7 Solving for a Direction-Specific Baseline 16
7.1 Introduction 16
7.2 Method 16
7.3 Results 17
7.4 Summary 19
8 NF_3 emissions across East Asia 20
9 RAC model analysis 21
9.1 Summary 21
9.2 Results 22
9.2.1 A '60% comparison' 25
10 Recent Publications 27

2 Executive Summary

2.1 Project Summary

Monitoring of atmospheric concentrations of gases is important in assessing the impact of international policies related to the atmospheric environment. The effects of control measures on chlorofluorocarbons (CFCs), halons and hydrochlorofluorocarbons (HCFCs) introduced under the 'Montreal Protocol of Substances that Deplete the Ozone Layer' are now being observed. Continued monitoring is required to assess the overall success of the Protocol and the implication for atmospheric levels of replacement compounds such as hydrofluorocarbons (HFCs). Similar analysis of gases regulated by the Kyoto Protocol on greenhouse gases will likewise assist policy makers.

Since 1987, high-frequency, real time measurements of the principal halocarbons and other radiatively active trace gases have been made as part of the Global Atmospheric Gases Experiment (GAGE) and Advanced Global Atmospheric Gases Experiment (AGAGE) at Mace Head, County Galway, Ireland. For much of the time, the measurement station, which is situated on the Atlantic coast, monitors clean westerly air that has travelled across the North Atlantic Ocean. However, when the winds are easterly, Mace Head receives substantial regional scale pollution in air that has travelled from the industrial regions of Europe. The site is therefore uniquely situated to record trace gas concentrations associated with both the mid-latitude Northern Hemisphere background levels and with the more polluted air arising from Europe.

The observation network in the UK has been expanded to include three additional stations; Angus near Dundee, Tacolneston near Norwich and Ridge Hill near Hereford. Ridge Hill became operational in February 2012, Tacolneston began operating in July 2012 and Angus Tower has been making measurements since late 2005.

The Met Office's Lagrangian atmospheric dispersion model, **NAME** (**N**umerical **A**tmospheric dispersion **M**odelling **E**nvironment), has been run for each 2-hour period of each year from 1989 so as to understand the recent history of the air arriving at Mace Head at the time of each observation. By identifying the times when the air, arriving at Mace Head, has travelled over un-populated regions, i.e. when the air has travelled across the north Atlantic and the air concentration reflects the mid-latitude Northern Hemisphere baseline value, the data collected have been used to estimate baseline concentrations, trends and seasonal cycles of a wide range of ozone-depleting and greenhouse gases for the period 1989-2014.

By removing the underlying baseline trends from the observations and by modelling the recent history of the air on a regional scale, estimates of UK, Irish and North West European (UK, Ireland, France, Germany, Denmark, the Netherlands, Belgium, Luxembourg) emissions and their geographical distributions have been made using **InTEM** (**In**version **T**echnique for **E**mission **M**odelling). The estimates are presented as yearly averages and are compared to the United Nations Framework Convention on Climate Change (UNFCCC) inventory.

The atmospheric measurements and emission estimates of greenhouse gases provide an important cross-check for the emissions inventories submitted to the UNFCCC. This verification work is consistent with good practice guidance issued by the Intergovernmental Panel on Climate Change (IPCC).

3 Overview of Progress

3.1 Update website

Atmospheric baseline concentrations for each gas reported at Mace Head have been estimated through to the end of April 2015 and are presented through the website:

www.metoffice.gov.uk/atmospheric-trends

The estimates for methane (CH_4) and nitrous oxide (N_2O) are presented in Figure 1 and Figure 2 respectively. Both show that the mole fractions of these gases are growing in the atmosphere faster than the long-term average.

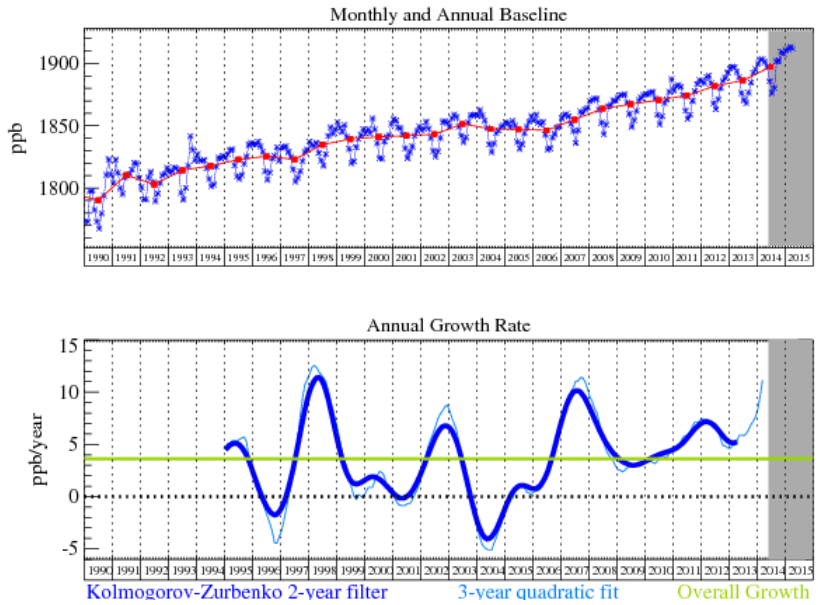

Figure 1: Monthly (blue) and annual (red) baseline estimate for the mid-latitudes in the Northern Hemisphere for CH_4 (top plot). Corresponding baseline growth rate estimated for CH_4 (lower plot) using 2 methods.

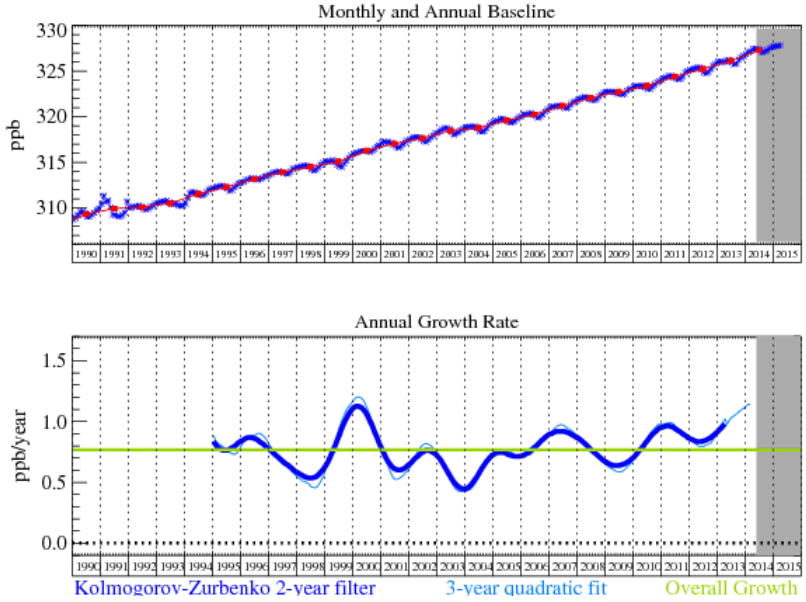

Figure 2: Monthly (blue) and annual (red) baseline estimate for the mid-latitudes in the Northern Hemisphere for N_2O (top plot). Corresponding baseline growth rate estimated for N_2O (lower plot) using 2 methods.

3.2 Investigating uncertainties in InTEM and the impact of using the different stations

The impact on uncertainty reduction on emission estimates of methane for the different Devolved Administrations (DAs) within the UK using different combinations of stations within the UK DECC network and also the two GAUGE tall towers has been investigated. The results are presented in this report

3.3 Direction specific baselines developed within InTEM

The concept of direction specific baselines has been developed within InTEM. 11 additional direction and height specific variables are solved for within the inversion. The prior baseline used is from the standard baseline estimation method for Mace Head. After the inversion each station has a specific and unique baseline that depends on where the air enters the model domain arriving at that particular station. The results of this work are presented in this report.

3.4 NF_3 emissions across East Asia

Nitrogen Trifluoride (NF_3) inversions have been performed for the first time across East Asia and are reported. The emissions estimates of NF_3 from South Korea are significant relative to the magnitude of the uncertainties.

3.5 RAC model analysis

The inventory refrigerant model has been provided by DECC for investigation on their behalf. The sensitivities of the model to the input parameters have been considered for the gas HFC-134a, the principle gas used as a mobile air conditioner, e.g. in cars. The results of this on-going analysis are presented.

4 Update on UK DECC network measurement sites

4.1 Mace Head (MHD)

The GC-MD performed reasonably well over the reporting period. The retention times of channel 1 and channel 2 species have a tendency to drift upward requiring periodic adjustment of the backflush balancing valve, particularly on channel 2. We have determined this is likely due to aging of the needle valves in the system and a full set have been ordered for replacement at the next convenient time.

The Mace Head Medusa-MS performed reasonably well over the reporting period. Since the installation of a new trap 2 on 14th May 2014, the rate of increase of the concentration of HFC-125 and HFC-32 in ambient air appears to have increased at a rate faster than indicated at other AGAGE sites. The problem may be associated with the high level of both these compounds in lab air and a leak, or leaks, in the system.

After testing, it was determined there were possible leaks on trap 1, Nafion 2 and a cross-port leak on V6. Blanks show no response for either of these compounds and, since all samples pass through the same flow path after V1, it's not clear why a leak would only affect air samples.

Repeated leak tests of the sample pump (spraying with P5 and checking for increased CH_4 on the MD) indicate no leak on the pump. The next step will be to take some flask samples from 10m concurrent with Medusa sampling and see if there is a difference in mixing ratios.

4.2 Tacolneston (TAC)

Operations at Tacolneston have continued with no major issues to report for the GC-MD or the Picarro-CRDS. The Medusa-MS has operated extremely well since the air conditioner was fixed. However, we do appear to have a source of SF_6 contamination, which as yet we have been unable to locate. It is fortunate that SF_6 is also determined via the GC-MD. Inter-lab comparisons were run on all three instruments between 23rd Mar 2015 and 25th Mar 2015.

4.3 Ridge Hill (RGL)

Operation of the Picarro-CRDS has continued with no issues in the last reporting period.

The GC-MD post-column was changed in February and following instrument optimisation N_2O data returned to 0.2% precision on the 27th of March (before the column change N_2O precision was 0.1-0.2%). SF_6 precision was unaffected by the column change. During the period when the instrument was being optimised the air sample module pump failed, as well as the thermostated lab extractor fan. Both were repaired by the 27th of March. The GC-MD is now operating well.

4.4 Angus (TTA)

Operation of the Picarro-CRDS at Angus continued with no major issues to report. A number of days data were lost due to the Picarro-CRDS pump failing on 25th Apr 2015. University of Bristol installed a replacement on 30th Apr 2015 and the Angus pump was brought back to UoB to be serviced. Cucumber inter-comparison cylinders were run on the Picarro-CRDS on 5th May 2015.

6 Assessing the Impact of the different stations in the UK DECC network

6.1 Introduction

A method has been developed to assess the impact in terms of uncertainty reduction of introducing observations from the 4 measurement sites in the UK DECC network. The sites have been introduced in the following order: Mace Head (MHD), Tacolneston (TAC), Ridge Hill (RGL) and Angus (TTA). CH_4 observations have been used as they are available at all of the sites for 2012-2014.

6.2 Method

The Bayesian framework and cost function have been used to assess the impacts. This framework has a rigorous mathematical method for estimating the uncertainty reduction due to the introduction of more knowledge, in this case more observations. It does have some limitations, namely that the errors are assumed Gaussian and that an initial emission estimate (prior) must be available. Also it is assumed that the uncertainties in the prior, the observations and the model transport are well characterised and known.

For this study we used the prior developed by Ganesan et al (2015) that uses the National Atmospheric Emissions Inventory (NAEI) (2012) UK emissions nested within European emissions. The European emission distribution is from EDGAR 2010 with the individual country totals scaled to UNFCCC 2012 values. The prior also contains a contribution from natural sources from a variety of different sources [Ganesan et al, 2015]. The relative uncertainty of the prior and the observations were also investigated.

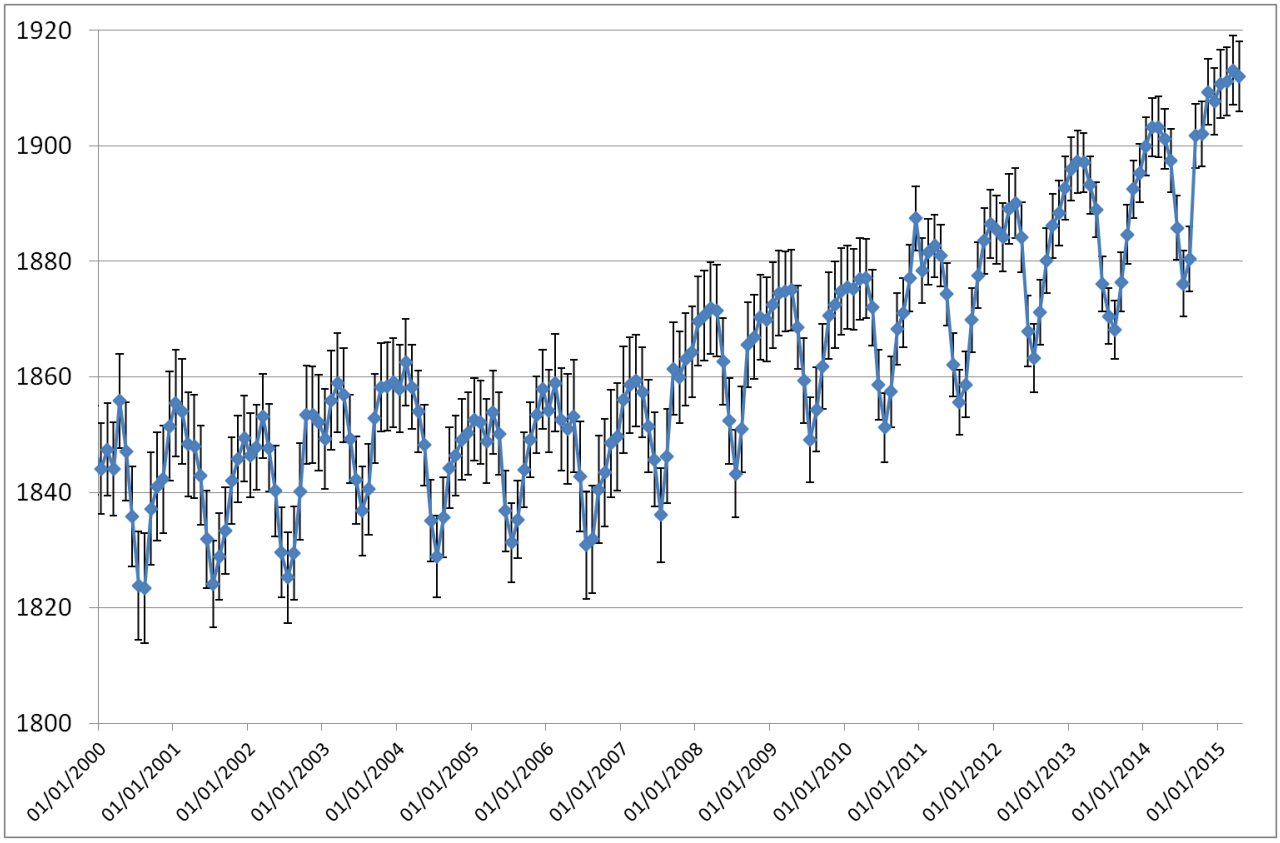

Figure 3: CH_4 monthly baseline mole fraction (ppb) as estimated from Mace Head observations 2000 – 2015. Baseline uncertainty (1 σ) shown.

The observation and model transport uncertainties follow the procedure described in previous DECC reports. In summary, the observation uncertainty is derived from a combination of repeatability uncertainty and aggregation uncertainty. The former is from the instrument and is the variability observed when the same tank of air is repeatedly measured. The latter is from the variability, standard deviation, in the observations when they are aggregated up to the modelling time period (2 hours). The CH_4 observations are measured at 1 Hz frequency at TAC, RGL, TTA (although there are regular data gaps as different heights are sampled) and 40 minute intervals at MHD. The model transport uncertainties are very difficult to quantify but are assumed to be related to the strength of the impact of very local emissions (high impact implies weak winds and low boundary layers and thus times when local un-modelled effects are strong) and the ability to estimate a good baseline mole fraction. The baseline is an estimate of the concentration of the gas in the air as it enters the inversion domain (See Figure 3). Both of these uncertainties are fully explained in previous DECC reports. The uncertainties are thus summarised:

- Observation ($\sigma_{precision}$ & $\sigma_{2h\ time\ period}$)
  - $\sigma_{precision}$ → Uncertainty due to repeatability of observation
  - $\sigma_{2h\ time\ period}$ → Uncertainty when observations aggregated to 2-hours

- Model ($\sigma_{baseline}$ & σ_{local})
  - $\sigma_{baseline}$ → Uncertainty of MHD baseline when applied to station observations
  - σ_{local} → Uncertainty increases as local influence increases

Usually: Model uncertainty >> Observation uncertainty

$$R = (\sigma_{precision})^2 + (\sigma_{2h\ time\ period})^2 + (\sigma_{baseline})^2 + (\sigma_{local})^2$$

In this work a new set of NAME runs were performed for the entire period for each station and for each observation height. Only the 90m and 100m CH4 observations were used from RGL and TAC respectively because of the close correlation between the observations from the different heights at the same station. Highly correlated observations need special treatment within the Bayesian framework. The 2-hr average observations were assumed for simplicity to be uncorrelated. The NAME particles were released in a 20 m vertical line centred on the height of the observation. Model particles within 40 m of the ground were assumed to be representative of the impact of the ground on the observation. 3-Dimensional meteorology from the Met Office at 17 (from July 2014) to 25 km horizontal resolution was used to drive NAME. The end points, in time and space, of each particle were recorded and were used to estimate the strength of the baseline from each of the different (11 in total) compass directions (WSW, WNW, NNW, NNE, ENE, ESE, SSE, SSW, Northern for particles between 6 and 9 km, Southern for particles between 6 and 9 km, and all particles above 9 km).

InTEM was used to estimate the emission strengths and magnitudes and also solved for the perturbation to the baseline dependant on the direction and height the model air entered the model domain. The latter thus develops the idea of a direction-specific baseline. This will be discussed later. The Bayesian framework has two components; a mis-match to the prior, and a mis-match to the observations. InTEM searches for the solution that minimises these mis-matches. The Bayesian cost function is described below:

$$y = (Me - o)^T R^{-1} (Me - o) + (e - e_p)^T B^{-1} (e - e_p)$$

M = Transport matrix (Number of times [t] x Number of grids [n]),
e = Emission estimate [n]
o = Observations [t]
R = Model-Observation uncertainties [t x t]
e_p = Prior emissions [n]

B = Prior uncertainty [n x n]

Uncertainty Analysis Matrix [n x n]

$$A = \left(M^T R^{-1} M + B^{-1} \right)^{-1}$$

From analysis of matrix A the uncertainty of each geographic region can be calculated.

InTEM was used to estimate the CH_4 emissions for each year 2012 – 2014 over a European domain. Estimates were calculated using the prior for 2012, MHD-only observations (Figure 4), then MHD and TAC observations (Figure 5), then MHD, TAC and RGL observations (Figure 6) and finally using all four sites (Figure 7). The UK estimates are presented below for each of the Devolved Administrations (DA) regions.

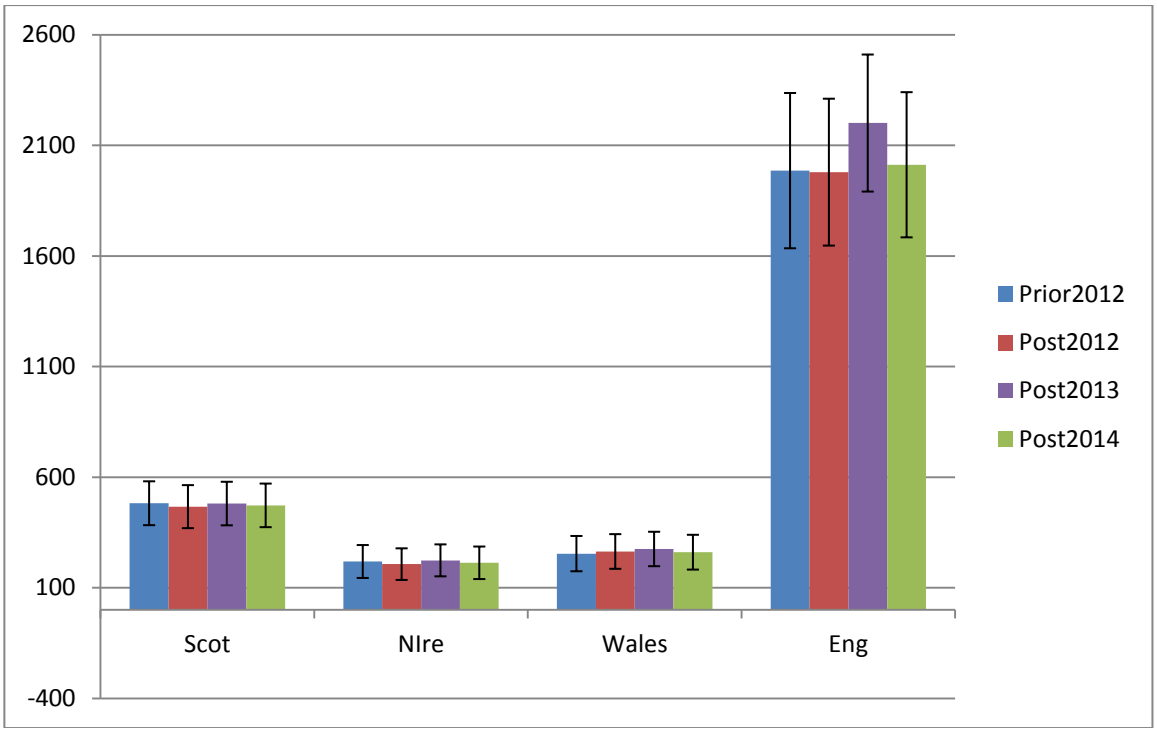

Figure 4: CH_4 emission estimates (1σ uncertainty) of the prior (2012) and from InTEM using MHD observations only for each DA for each year 2012 – 2014 (kt/yr).

The MHD-only inversions (Figure 4) show very little uncertainty reduction across the DAs. Every year shows a small decrease in the uncertainty but this reduction is not visible in Figure 4. In the standard non-Bayesian InTEM setup (with just MHD data) three years of data are used rather than just a single year as in this experiment. Using three years of MHD data, England's emission uncertainty reduced from 18% with the prior (1990 ± 350 kt/yr) to 14% after the inversion and the English total was estimated to be 2080 ± 290 kt/yr.

When TAC data are included (Figure 5) there is a clear reduction in uncertainty in each of the years 2012-2014 from 18% to 10-12% for England but little reduction for the other three DAs. The data suggest that the prior emissions for the England are too high, the mean prior value is 1986 kt/yr, whereas the mean InTEM estimate over the 3 years is 1851 kt/yr, although the uncertainties overlap. It is interesting to note that the posterior uncertainty for England in 2012 is larger than the other two years. This is to be expected as TAC data only became available in the second half of the year (July 2012).

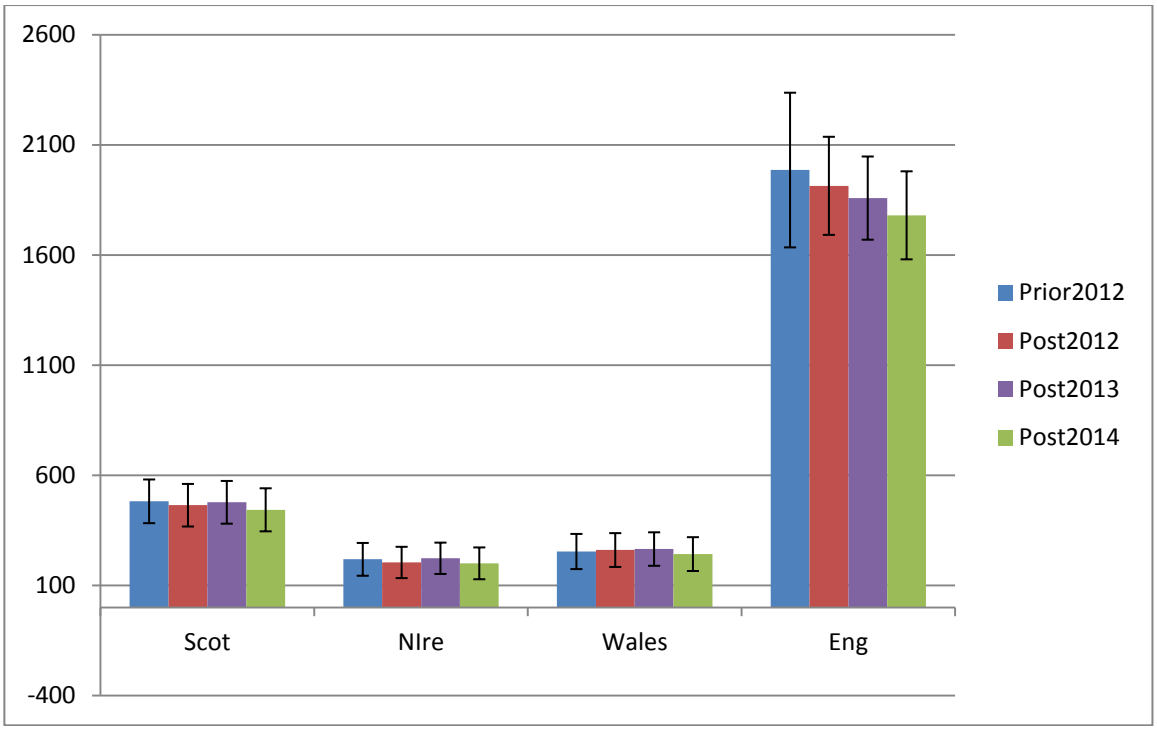

Figure 5: CH_4 emission estimates (1σ uncertainty) of the prior (2012) and from InTEM using MHD and TAC observations for each DA for each year 2012 – 2014 (kt/yr).

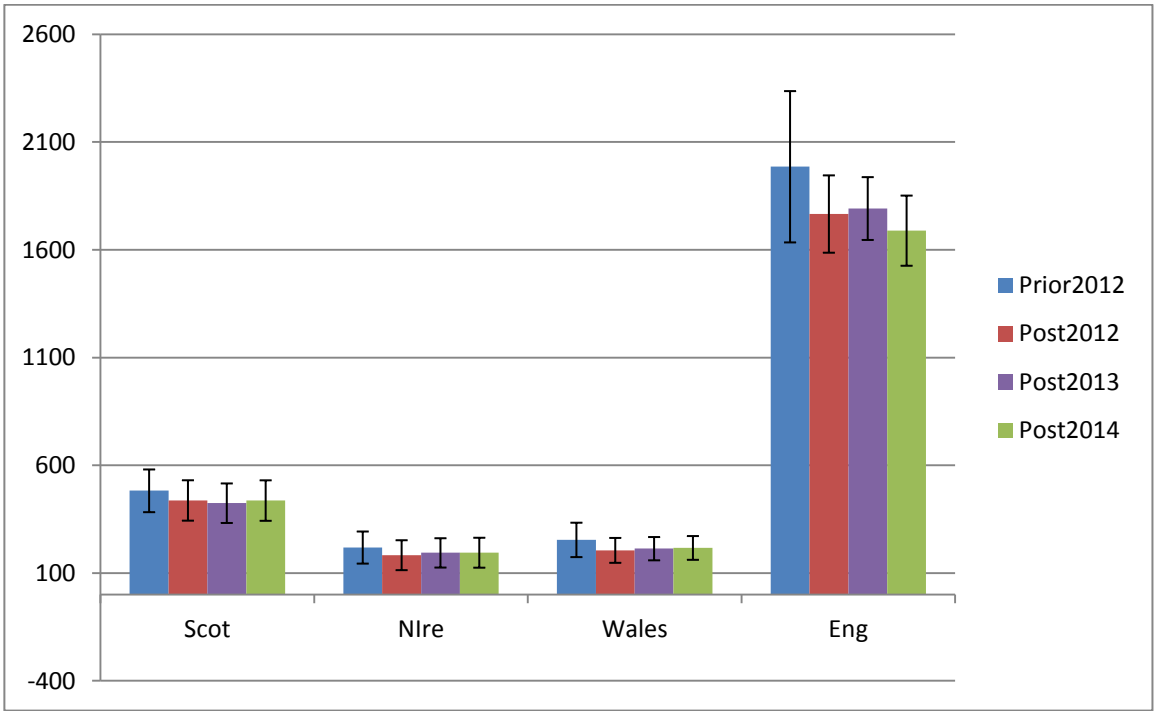

Figure 6: CH_4 emission estimates (1σ uncertainty) of the prior (2012) and from InTEM using MHD, TAC and RGL observations for each DA for each year 2012 – 2014 (kt/yr).

The inclusion of RGL (Figure 6) shows an additional reduction in uncertainty for England from 18% to 8-10%. There is now a discernible reduction in uncertainty for the estimates for Wales from 31% to 25-28%. There is little impact in either Northern Ireland or Scotland. Also the inversion results show a reduced emission estimate for England and Wales compared to the prior.

Figure 7 shows the uncertainty reduction achieved by using the data from all of the UK DECC network stations. Uncertainty reduction is seen in three of the four of the DAs (England 18% to 7-

9%, Wales 31% to 23-29%, and Scotland 21% to 16-18%). The most significant change from the 3 station experiment is the impact in Scotland. Across the DAs the inversion results indicate a reduced emission compared to the prior (InTEM UK emissions 18-20% lower) although there is overlap in the 1σ uncertainty estimates.

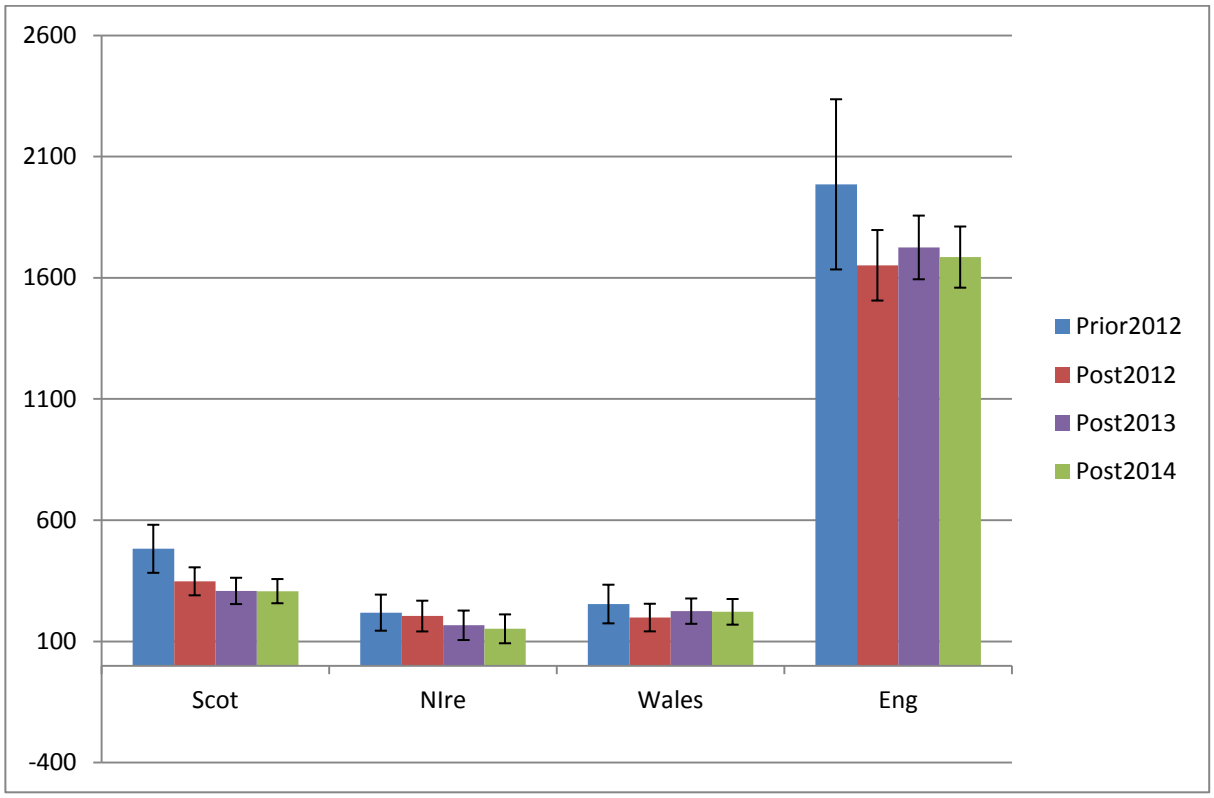

Figure 7: CH_4 emission estimates (1σ uncertainty) of the prior (2012) and from InTEM using MHD, TAC, RGL and TTA observations for each DA for each year 2012 – 2014 (kt/yr).

For comparison InTEM was also used to estimate CH_4 emissions with a weaker prior (increase prior uncertainty to 250% from 200% per 25 km grid) and more certain observations (model-observation uncertainty halved). The results of this comparison for England are summed up in Figure 8. The results denoted with the letter (a) are as shown in Figure 4 to Figure 7, the results denoted by the letter (b) are the new estimates with the weaker prior and stronger observational certainty. It is interesting to note that with more observations (through adding more stations) or stronger observational certainty (and weaker prior certainty) decreases the emission estimates for England (and the UK) although there is little change between the 3-, and 4-site inversions.

The analysis was further expanded by also including data from the two GAUGE stations, Heathfield (HFD) (in Sussex) and Bilsdale (BLD) (in North Yorkshire), in a 6-site inversion. The uncertainty reduction for England in the 6-site network (2014 only) is very similar to the 4 UK DECC network inversion results. The emission estimate maps for 2014 for the prior, 1 – 4 site, and 6 site inversions are shown in Figure 9 - Figure 14. The addition of each extra station does improve the resolution of the emission estimate especially close to the new station.

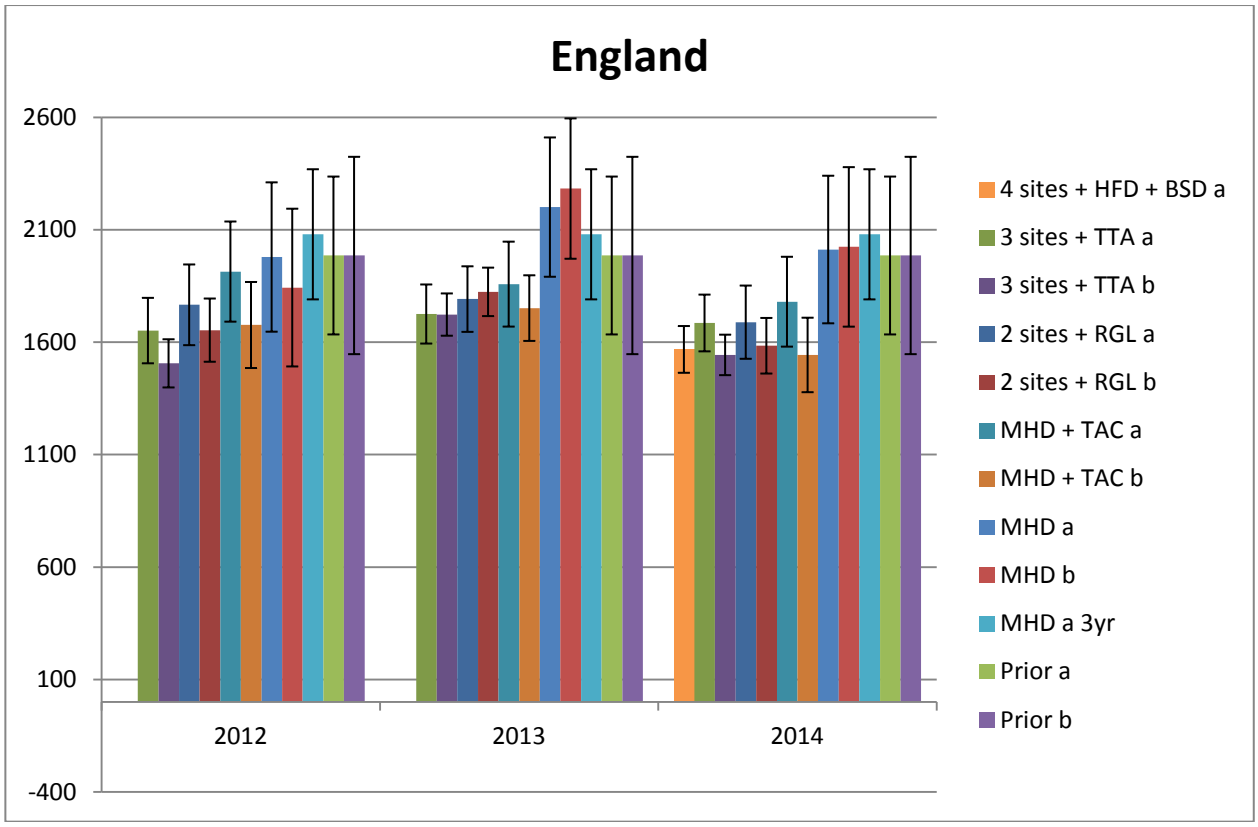

Figure 8: CH_4 emission estimates (1σ uncertainty) for England for 2012, 2013 and 2014. The plot shows the results from 5 combinations of stations (MHD, TAC, RGL, TTA, HFD and BSD). (a) denotes the first InTEM experiment as shown in Figure 4 - Figure 7, (b) second InTEM experiment with increased prior uncertainty and reduced model-observation uncertainty (kt/yr).

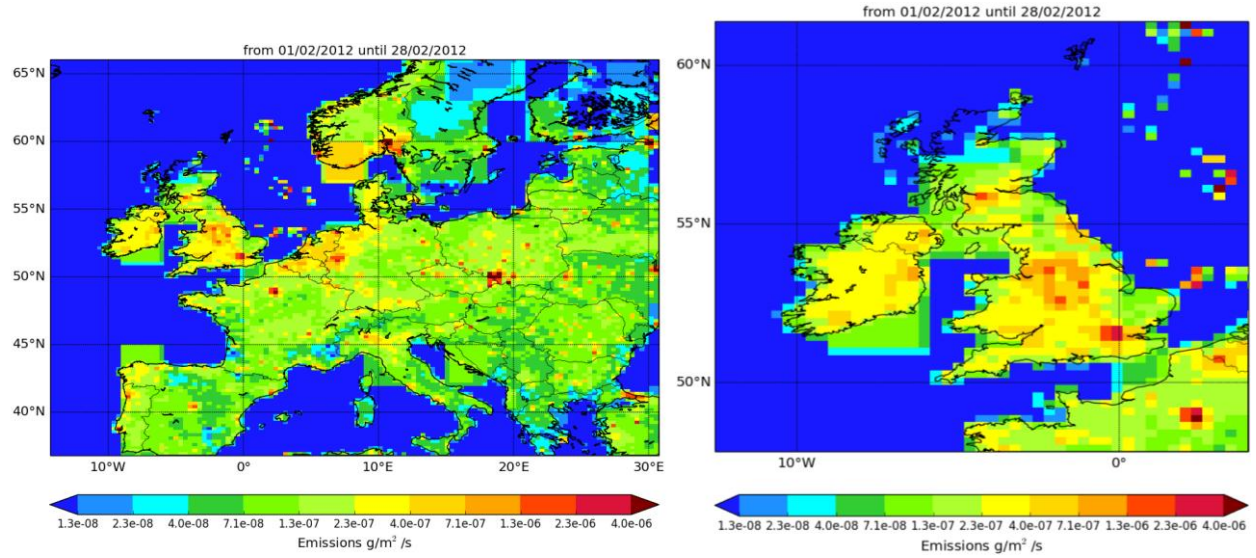

Figure 9: Prior emission estimate for CH_4, combining NAEI in the UK with EDGAR scaled to UNFCCC estimates for the rest of Europe, interpolated to the 25 km grid used in InTEM. Right hand plot is zoomed in to the UK.

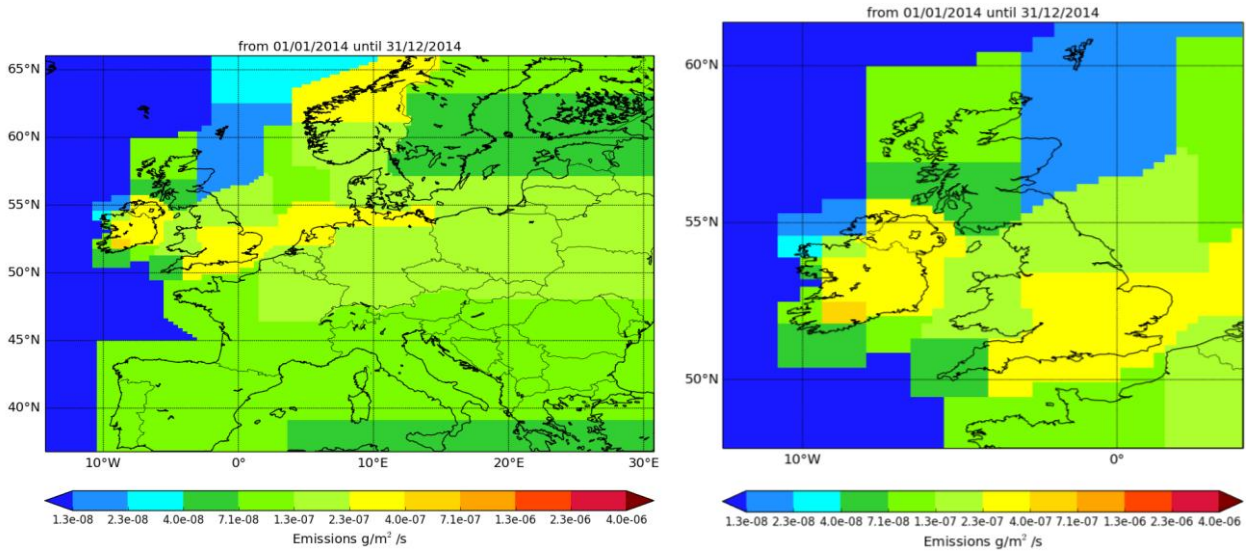

Figure 10: MHD-only InTEM emission estimate 2014 for CH_4. Right hand plot is zoomed in to the UK.

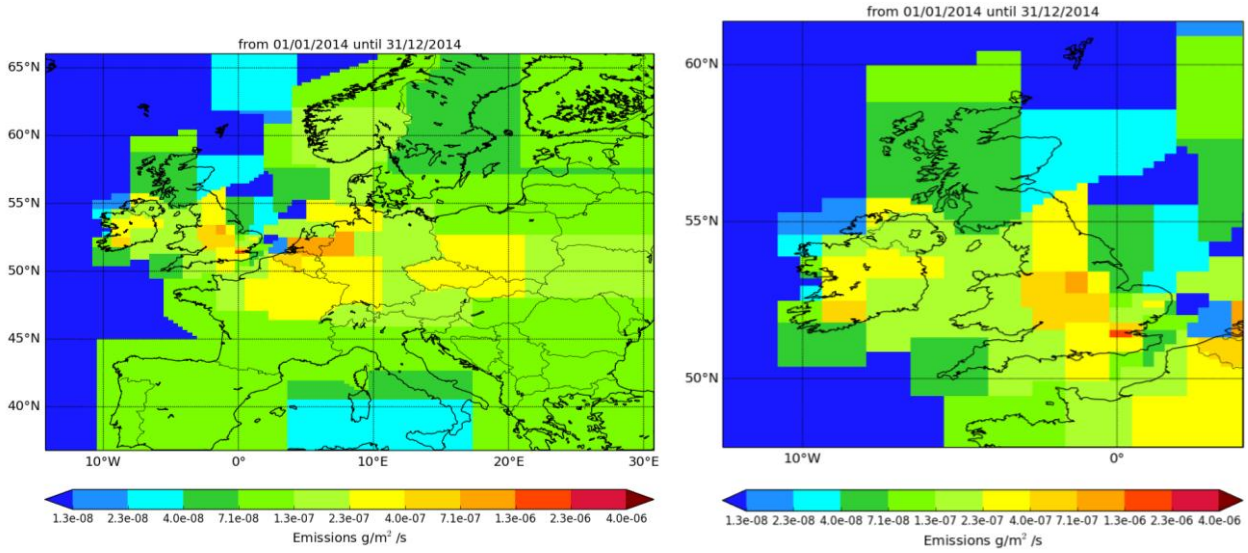

Figure 11: MHD and TAC InTEM emission estimate 2014 for CH_4. Right hand plot is zoomed in to the UK.

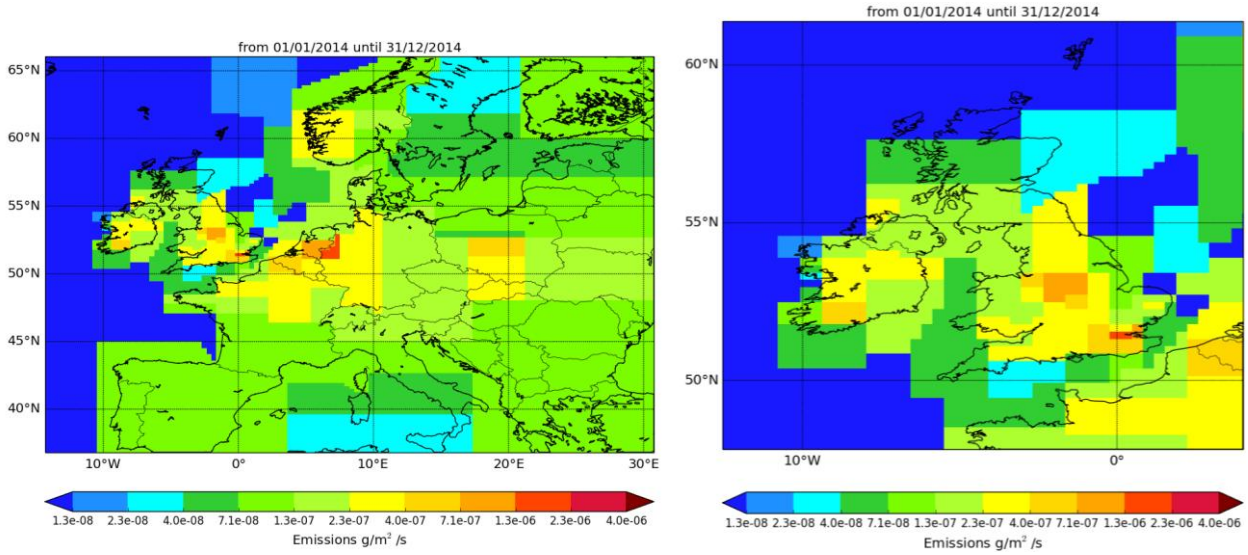

Figure 12: MHD, TAC and RGL InTEM emission estimate 2014 for CH_4. Right hand plot is zoomed in to the UK.

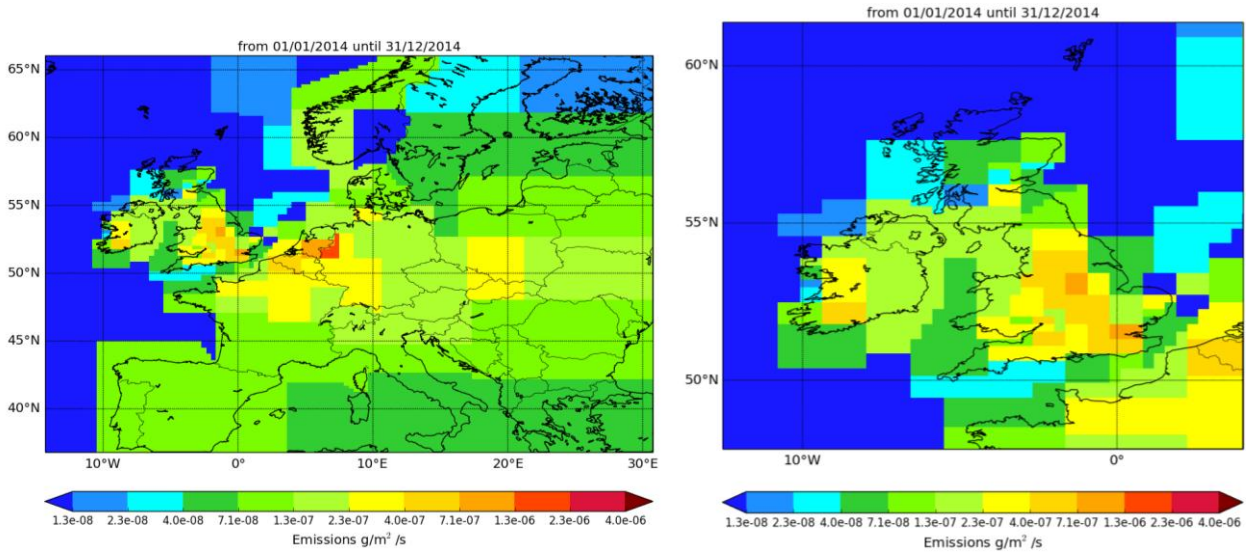

Figure 13: MHD, TAC, RGL and TTA InTEM emission estimate 2014 for CH_4. Right hand plot is zoomed in to the UK.

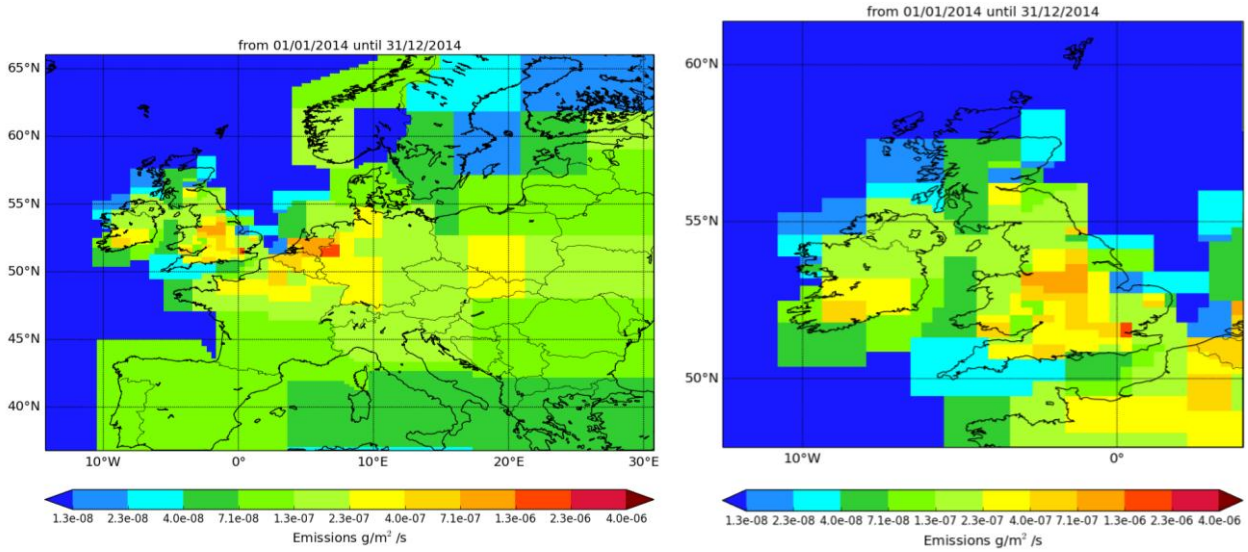

Figure 14: MHD, TAC, RGL, TTA, HFD and BSD InTEM emission estimate 2014 for CH_4. Right hand plot is zoomed in to the UK.

6.3 Summary

The UK DECC network has been shown to add value to the DA emission estimates for CH_4. The results are summarised in Figure 15. The additional stations allow the inversions to be conducted on annual (or smaller) time intervals rather than the previous 3-year periods. Each station adds detail around its region of influence. TAC significantly improves the resolution achievable across England (the number of grids representing England increases from 5 to 31 through adding TAC), RGL across Wales and England (the number of grids representing England and Wales increases from 31 to 46 and 1 to 7, respectively, through adding RGL to the 2-site network), and TTA across Scotland (the number of grids representing Scotland increases from 5 to 24 through adding TTA to the 3-site network). The two GAUGE stations, on an annual time-frame, do not significantly alter the English emission estimates but do give greater clarity to London and the North East. They would also allow smaller (sub-annual) time windows to be investigated.

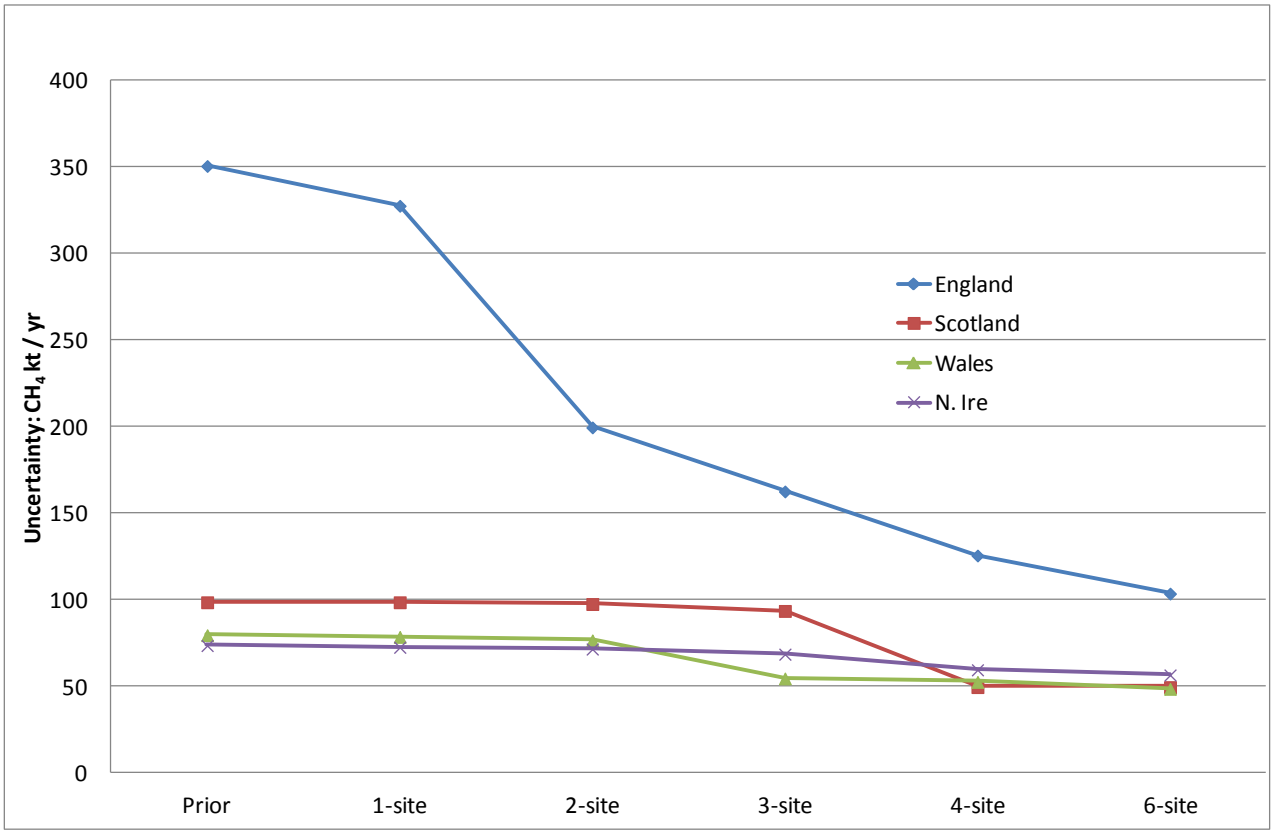

Figure 15: Uncertainty estimates (experiment a) of CH4 (kt/yr) for the four DAs using the prior and 1- to 6-site inversions.

7 Solving for a Direction-Specific Baseline

7.1 Introduction

With the introduction of a network of stations it is necessary to define a baseline for each of the stations across the network. A baseline for each station cannot be estimated in the same way as currently done for MHD because the other stations within the network do not receive air that is unaffected by UK (and regional) emissions. Initially the MHD baseline was used across the network as a good first approximation. However this approach has limitations because each station does not always receive air from the same direction as Mace Head at the same time. For example TAC may be observing air from the north at the same time as MHD is observing air from the south-west. The impact of air from the upper troposphere is also important and is variable across the network at different times. The mole fraction of a gas usually has a vertical and latitudinal gradient due to heterogeneous emissions. It is therefore important to reflect these differing baselines within the inversion system and a method has been developed that directly solves for an adjustment to the MHD baseline depending on the direction and height the air entered the regional modelled domain.

7.2 Method

The direction and height the air enters the regional modelled domain has been recorded for each 2-hour period 1989 – May 2015 for each station when observations were made. This required a completely new set of NAME runs to be undertaken and modifications to NAME itself. This information was interrogated and the percentage contributions from 11 different directions and heights for each 2-hour period for each station were determined. The 11 directions are: WSW, WNW, NNW, NNE, ENE, ESE, SSE, SSW (all below 6 km); From the south 6-9 km; From the North 6-9 km; Above 9 km. Figure 16 shows a schematic of the different directions used within InTEM.

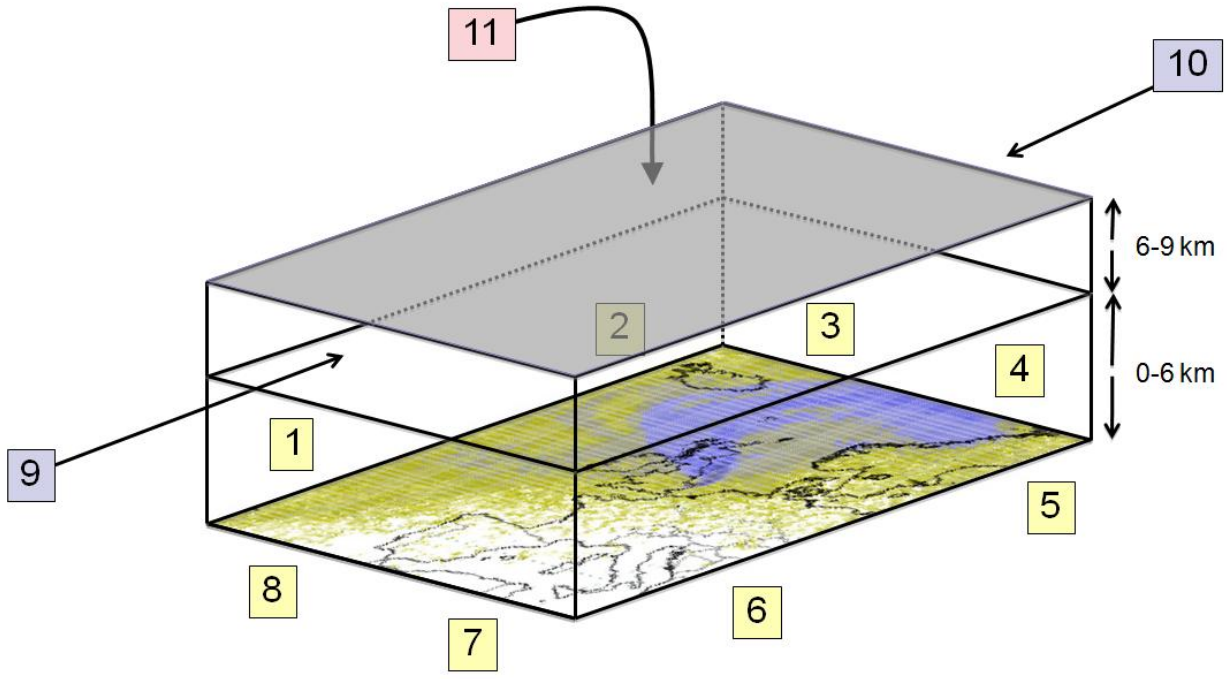

Figure 16: Schematic of the 11 different directions used within InTEM.

InTEM was modified to use this information to adjust the MHD baseline (defined as the prior baseline) separately for each of the 11 directions as part of the inversion process.

7.3 Results

The results here relate to the InTEM inversion for CH_4 as discussed in the previous section for 2014 using all of the 4 UK DECC network stations and the 2 GAUGE stations, Heathfield and Bilsdale. Table 1 shows the posteriori results after the inversion. These results are applicable across the network. The actual posteriori baselines at each station will vary at the different stations because the contributions from the 11 directions will vary in time site to site. It is important to note that the CH_4 Northern Hemisphere mole fraction in 2014 was around 1880 ppb so 1% (0.01 multiplying adjustment) relates to a mole fraction adjustment of 18.8 ppb. Therefore the 0.972 adjustment for upper tropospheric air generates a negative adjustment of around 53 ppb.

Direction	Posterior Multiplying Factor
WSW	0.995
WNW	1.001
NNW	0.998
NNE	1.003
ENE	1.008
ESE	0.991
SSE	0.982
SSW	0.980
6-9km South	0.980
6-9km North	0.982
Above 9km	0.972

Table 1: Posteriori direction specific baseline multiplying factors.

Figure 17 - Figure 19 show the prior (black) and posterior (red) baseline estimates at MHD, TAC and RGL respectively. The prior baseline is identical in each case. Similar plots can be created for the each of the other stations (TTA, HFD and BSD) but all show essentially the same patterns. On the whole the posterior baselines are lower than the prior baseline although there are times when the mole fractions are elevated, most notably when the air is from the north. There is no particular reason why the baseline would, on the whole, be lower, it will be interesting to investigate whether this is a general pattern seen in the majority of gases or whether this is specific to methane. Solving the baseline adjustment variables only once for the entire year is potentially a limitation as there will be seasonal variations in the latitudinal and height gradients.

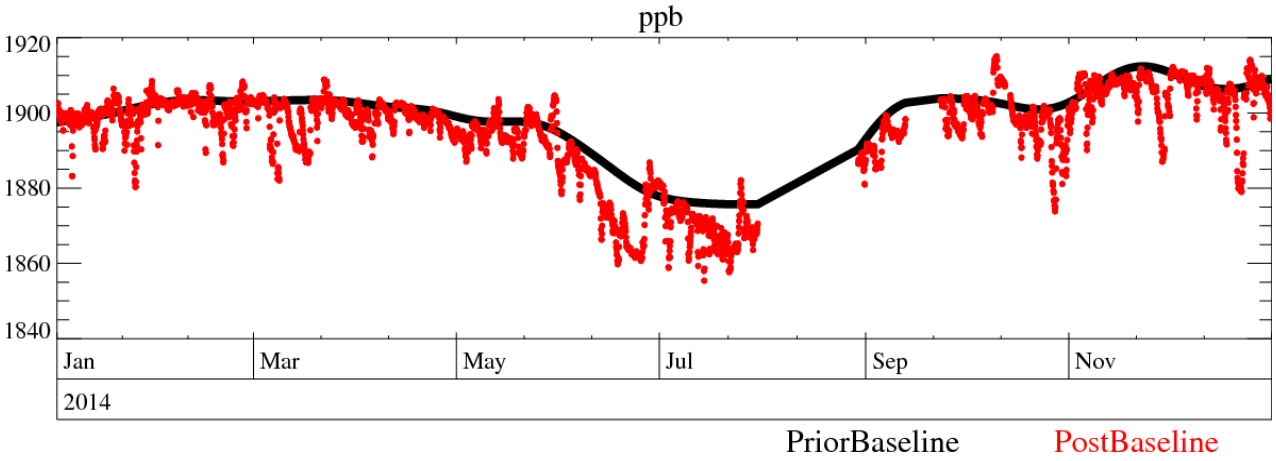

Figure 17: Adjusted MHD baseline (red) for CH_4 for 2014. The black line shows the prior MHD baseline.

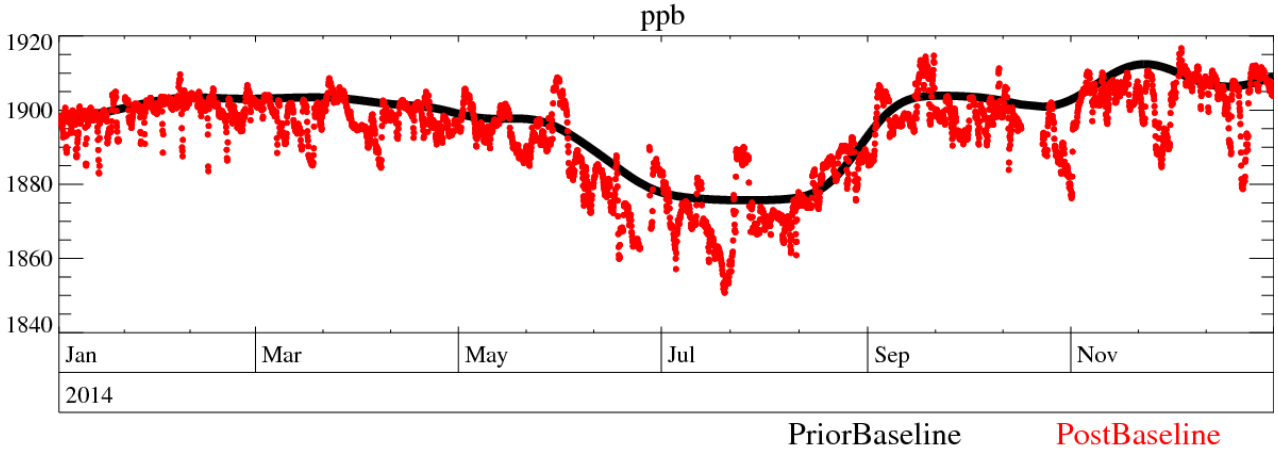

Figure 18: Adjusted TAC baseline (red) for CH_4 for 2014. The black line shows the prior MHD baseline.

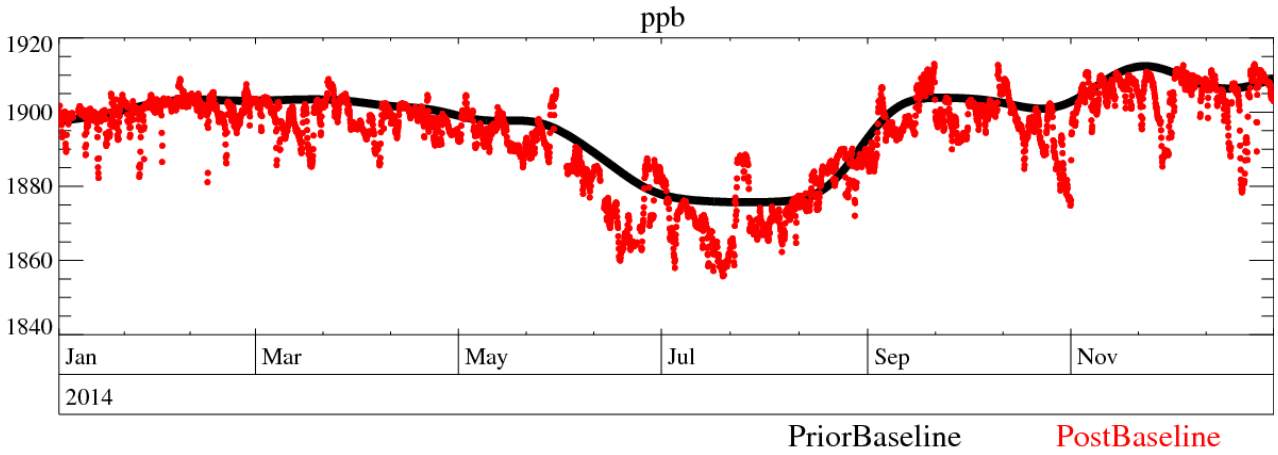

Figure 19: Adjusted RGL baseline (red) for CH_4 for 2014. The black line shows the prior MHD baseline.

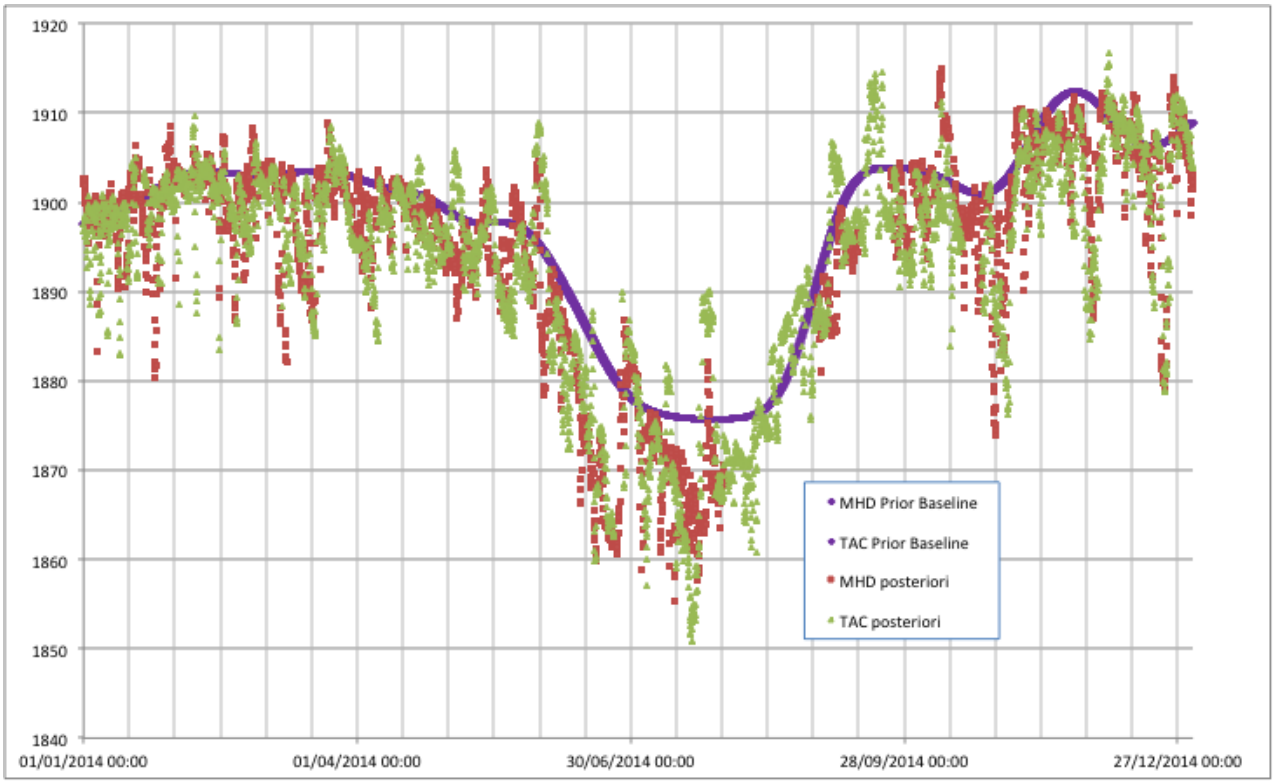

Figure 20: Comparing prior CH_4 baseline for 2014 with the posteriori baselines from MHD and TAC (ppb).

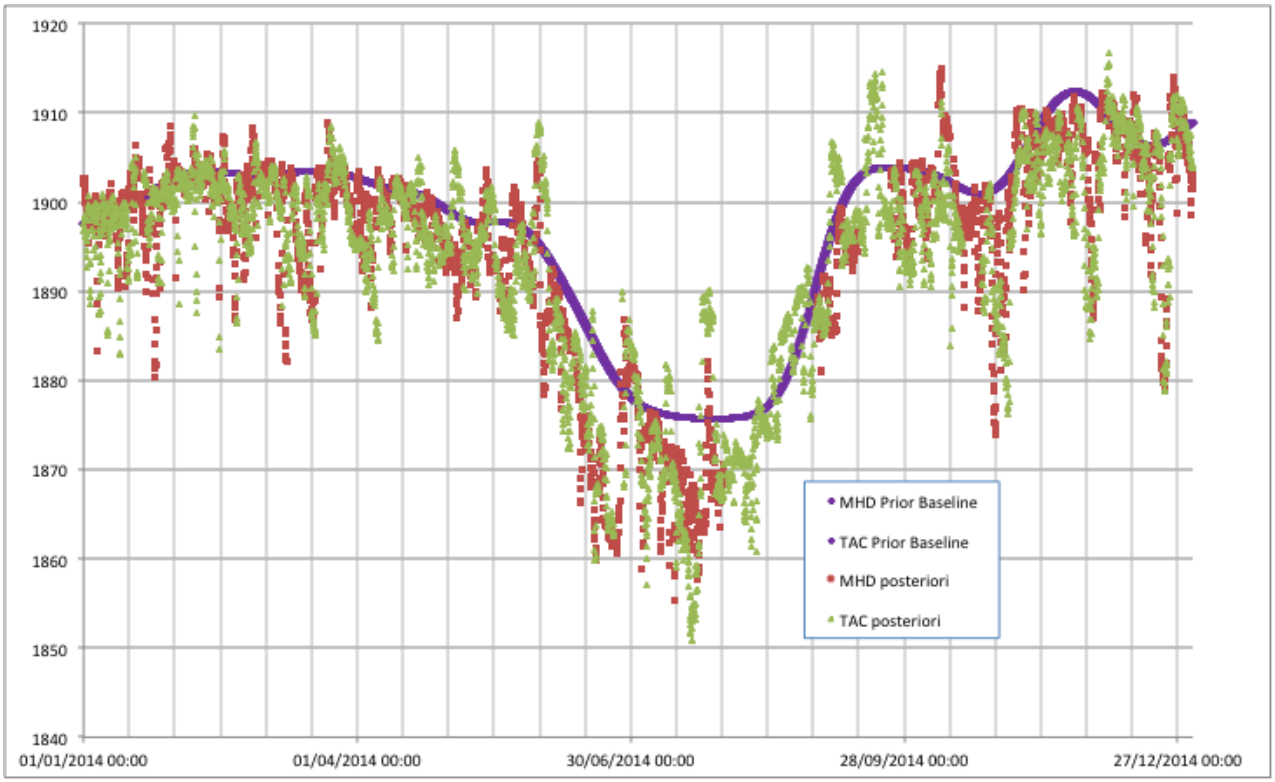

Figure 20 shows the comparison between the prior baseline from the MHD observations (identical at both sites) and the post-inversion (posteriori) baselines estimated at MHD and TAC. The values used for the different directions are shown in Table 1. The estimated baselines at MHD and TAC are different showing the varying contributions of air from different compass and height directions at matching times at the two stations. The summer-time minimum is, on the whole, further reduced by the inversion at both stations, however there are times when the baselines are

elevated compared to the prior, most notably when the air has come from the north east (adjustments greater than 1).

7.4 Summary

A direction specific baseline has been added to the inversion process within InTEM. It solves for 11 additional variables, multiplying factors applied to the prior MHD baseline depending on the location and height of the air entering the model domain, that allow for a location specific baseline to be estimated. This is important as the observed gases have horizontal and vertical gradients and the histories of the air from the different stations are different.

The results show that the direction specific baselines vary from station to station as expected, and that the air from elevated positions or from southerly latitudes, have lower CH_4 mole fractions.

8 NF_3 emissions across East Asia

Nitrogen Trifluoride (NF_3) inversions have been performed for the first time for the East Asian region using data from the Gosan AGAGE station on Jeju island, South Korea. The results show that this region, unlike Europe, is a significant emitter of NF_3 and with South Korean emissions dominant. Prior information was taken from the Edgar database v4.2. The posteriori emissions show very large deviations from those 'bottom-up' estimates. Distinct areas of NF_3 emissions within South Korea and Japan could also be located with significant certainty in the inversion (Figure 21).

The baseline concentrations were solved for within the inversion (as detailed in the previous section), utilising measurements from other AGAGE stations (at Mace Head and Cape Grim) to estimate the concentration of air arriving from the edges of the inversion grid. Significantly, the baseline can now be estimated for periods when air masses are arriving at Gosan from the Southern Hemisphere as these is described by the baseline directions 7, 8 and 9, allowing the inversion to utilise all available data (Figure 22). Previously all observations made when the air came from the south were not used because the inter-Hemispheric gradient in concentration is so strong and regularly seen when the air flow is from the south.

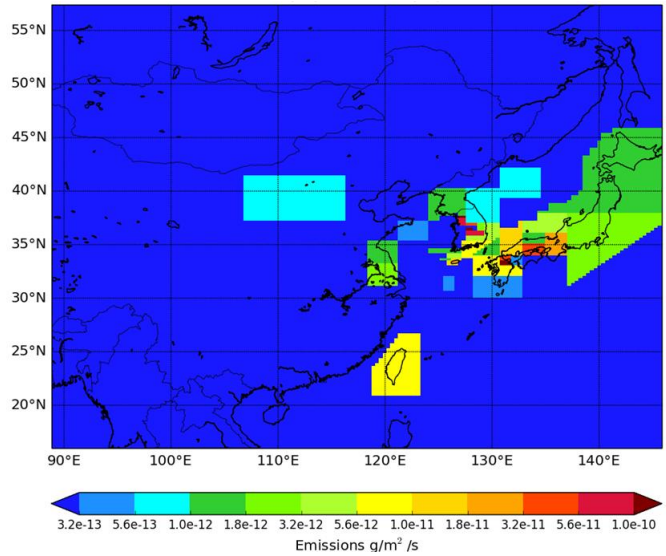

Figure 21: Map of the East Asian InTEM inversion domain showing the areas of high NF_3 emissions.

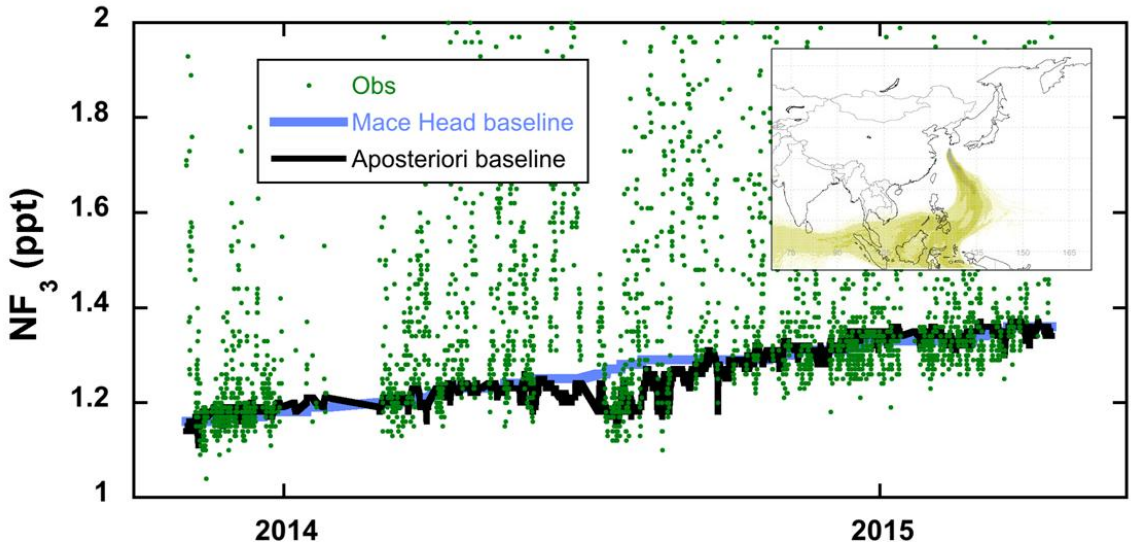

Figure 22: Timeseries and estimated baseline for NF_3 at the Gosan AGAGE station, South Korea. Pollution episodes reached over 20 ppt, however, the estimated baseline deviated

significantly below that at Mace Head due to air masses arriving from the Southern Hemisphere (see inset map) during the summer months.

9 RAC model analysis

9.1 Summary

Following provisional analysis of the Refrigeration and Air-Conditioning (RAC) model by the University of Bristol (UoB), two key inputs were highlighted as potential key contributors to model output variability. With these parameters (RAC 12/13 refill assumption and penetration rate) identified, objectives defined in the last DECC report were used to determine the combined influence of these parameters and scope for modification of the input device via one of two potential methods: development of the current RAC model in its native Excel/Visual Basic format, or extraction of the relevant sectors of the model into a new environment, namely the programming language Python. Considering current in house knowledge and the possible efficiency improvements, Python was chosen.

With a UK emissions contribution exceeding 60% of the total emitted volume of HFC-134a, Mobile Air-Conditioning units (MAC) are the dominant source of emission from RAC sectors. MAC units are most commonly found fitted to non-commercial automobiles (light mobile air-conditioning, LMAC), but are also found in other vehicles: buses, commercial vans and trains (other mobile air-conditioning, OMAC). While less common, these units may comprise a significantly larger charge size, and hence a greater volume of potential emissions per unit.

In the provisional analysis of the RAC model, which focussed primarily on RAC sectors 12 (LMAC) and 13 (OMAC), the most influential variable was determined to be the refill parameter. This input variable, provided as a YES/NO macro, is used to provide an assumption on the refill trends of automobiles in the fleet. Throughout its usable lifetime, any given unit suffers from a degree of refrigerant leakage which, over time, depletes the total charge volume. When the refill parameter is set to ‘YES’, it is assumed that every unit in the UK fleet is ‘topped-up’ on an annual basis. Conversely, when set to ‘NO’, it is assumed each unit charge degrades steadily throughout its lifetime until disposal, with no top-up.

The refill parameters lack of flexibility means it is unlikely to accurately represent the state of UK MAC refill trends. While undoubtedly a percentage of the UK vehicle fleet does benefit from annual MAC refill (with a small number likely to be filled on an even more regular basis), it is also likely that a significant portion of the fleet is not replenished annually (research indicates vehicle manufacturers recommend refill at 2 year intervals). With this is mind, and with an aim to explaining the large discrepancy between bottom-up figures (DECC, reported to the UNFCCC) and top-down emission estimates generated by the Met Office (employing the NAME atmospheric dispersion model and atmospheric observations from the UK and Ireland), the raw data and calculation methodology of RAC sectors 12 and 13 were transferred from the original model into the Python programming domain.

Modelling in Python offers a number of advantages over traditional methods based on spreadsheet functionality. Perhaps most importantly for this study, transferral to python allows the refill input to be redefined. For this work, the YES/NO input has been replaced by a percentage input variable. When set to the maximum (100%), all units are assumed to be refilled annually; likewise, the minimum value (0%) assumes no refill throughout lifetime. Uniquely, the extracted section of the model now accepts any input value as a percentage (including values in excess of 100%, representing refill frequencies in smaller than 1 year). Rather than a simple interpolation of results between 0 and 100% refill, the newly developed Python routine applies the percentage input to the total number of MAC units in each year, splitting these inputs and subjecting the resultant values to the required calculations (operating and disposal loss calculations differ based on whether the unit is refilled or not). In future work, this may be modified further to allow for multiple refill scenarios, whereby individual units may be topped-up any number of times during their lifetime (annually, every two years etc.).

Aside from the additional flexibility of input variables, Python offers significant improvements in terms of processing speed. At current, the RAC-12 function; that is, the Python script which calculates LMAC emissions, determines output for a single selected species (HFC-134a by default), while the original model calculates for all species in each sector. Nevertheless, RAC-12 emissions are now calculated in 15.64ms. Even if all possible species (the RAC model has 22 possible chemicals listed, with only three used in the LMAC sector) were calculated in turn, the process would take approximately 0.34s. In contrast, the current RAC model's average RAC-12 processing time is 42.38s: 124 times slower than the Python equivalent. When a large number of model runs are required to test sensitivity to individual/combined variable modifications, Pythons vastly improved processing speed is invaluable.

As a secondary advantage, the RAC Python functions are tailored to accept raw inputs as CSV (comma separated value) files. While perhaps a basic data platform, CSV format allows complete flexibility in terms of annual values. In comparison, the original RAC model takes values at set intervals (i.e. decadal) and linearly interpolates the remaining values, offering little scope for testing individual scenarios during certain years.

9.2 Results

The discrepancy between National Inventory derived UNFCCC and independent top-down (Met Office) emission estimates has been well documented in an earlier DECC report (DECC 6 month report, May 2014-Oct 2014, submitted Nov 2014). Here the top-down estimate is presented as a solid red trend line (1995-2013) with related error bars, while the UNFCCC estimates are shown as a dashed black line.

The earlier report highlighted the total variability provided by the refill parameter. It is presented again here; model runs were conducted for a complete range of refill percentages in 10% intervals. The total annual estimate range is plotted as a shaded region in Figure 23. For comparison, the variability incurred as a result of changing RAC-12 (LMAC) unit lifetime (within the recommended limits) is also shown below.

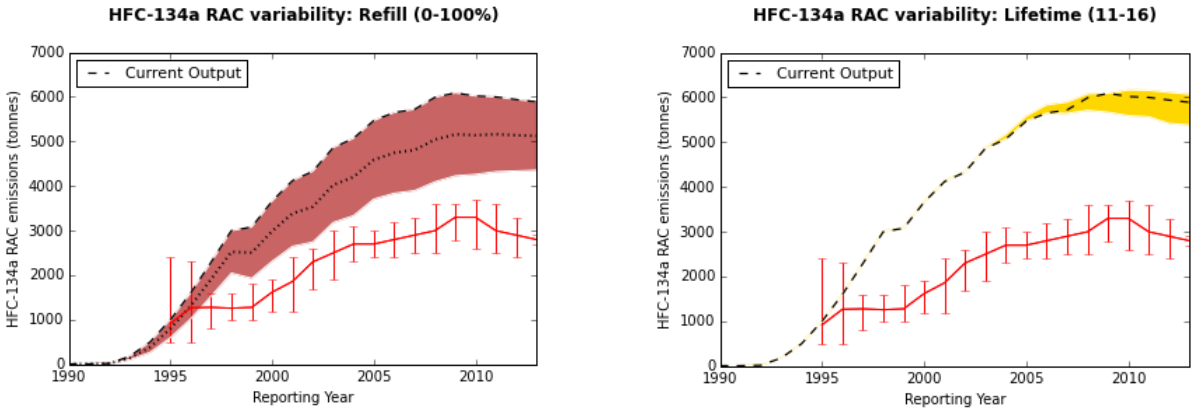

Figure 23: Potential HFC-134a emissions 1990-2013 a) As a result of varying the refill parameter (0-100%), limits indicated by the shaded maroon area and b) As a result of varying the lifetime parameter (11-16 years), limits indicated by the shaded yellow area. The dashed black line indicates current estimates, the solid red line indicates the Met Office top-down estimates and the dotted line (left) indicates a 50% refill rate

As seen in Figure 23, changing the default refill setting from 100% to 0% results in a theoretical emissions reduction of approximately 2 Gg (1Gg = 1000 tonnes) in 2010, equivalent to a third of the total inventory. While an assumption of no refill is implausible, so is the current conservative position of 100% refill, therefore allowing for a refill rate between the extremes will represent a more accurate picture from this sector. What the actual refill rate is, and how to estimate it, is the next challenge. The dotted line indicates the emission estimate trend generated by assuming a

1:1 ratio of units refilled to units not refilled (50% refill rate). As seen, this still equates to a >1 Gg difference in estimates (2010, revised vs. original UNFCCC submission). For comparison, the Figure 23 plot b) shows total variability in emissions estimate with changing lifetime. Even at the extremes of the lifetime range (maximum 16 years, minimum 11 years, default 15 years), the total theoretical reduction does not exceed 0.5 Gg in any given year.
Through rapid model output, the updated RAC sectors allow for efficient evaluation of combined input variability. Figure 24 combines a complete suite of model runs combining refill variability (0-100% in 10% intervals) with all RAC-12 (LMAC) unit lifetime possibilities (11-16 years).

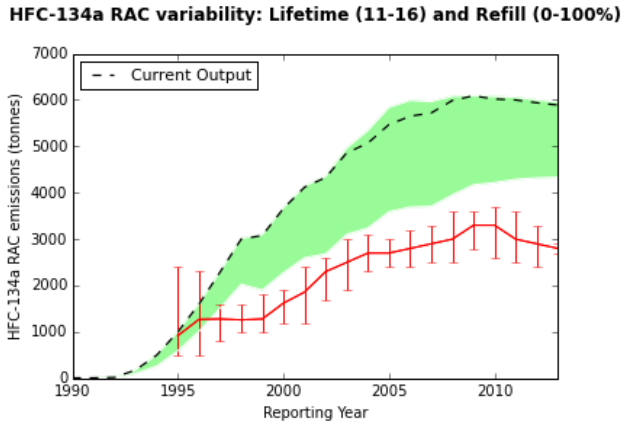

Figure 24: The combined theoretical variability in total HFC-134a emissions arising as a result of RAC-12 refill and lifetime sensitivity tests. The dashed black line indicates current estimates and the solid red line indicates the Met Office top-down estimates.

Owing to the minor sensitivity of changes in lifetime to the total emissions estimate, the variability is dominated by changes in the refill parameter. However, despite the potential for estimate reductions, there is still a notable divergence between top-down and bottom up figures, after 1997. Combining a refill input of 50% (half of the UK automobile fleet assumed to be refilled annually) with a unit lifetime of 11 years yields a 2013 estimate of 5.4 Gg, 1Gg lower than the published estimate but still over 2.6 Gg higher than the top-down method, and well outside of the respective error bars. Even when employing the most conservative variable inputs (0% refill and a unit lifetime of 11 years), a 1.5 Gg difference separates estimates, suggesting the documented divergence cannot be explained (at least solely) by refill assumptions.

Alongside refill rate, the original DECC report highlighted penetration rate as a variable whose modification had the potential to notably influence the final annual emission estimates. In our rebuilt section of the RAC model, penetration rate is input via CSV file, meaning each value may be modified independently. Penetration describes the percentage of automobiles which, in their original state, were fitted with an air-conditioning system.

Within the CSV input file, each individual penetration rate may be subject to scrutiny. Default penetration rates sit at 5% in 1990, increasing to 80% in 2008, reflecting increased demand and improved manufacturing technologies. All other values are calculated via a simple linear interpolation, assuming a linear increase in the number of UK automobiles fitted with a MAC unit. Penetration assumptions, included in the ICF International report, are provided by refrigerant producers and independent research; as with other inputs, the penetration rates are subject to a range of assumptions which create uncertainty. In order to test the influence of penetration rate on output values, the default values were lowered: from 5 to 1% in 1990 and 80 to 60% in 2008. Other years were calculated using the same method as implemented in the original RAC model, a simple linear interpolation.

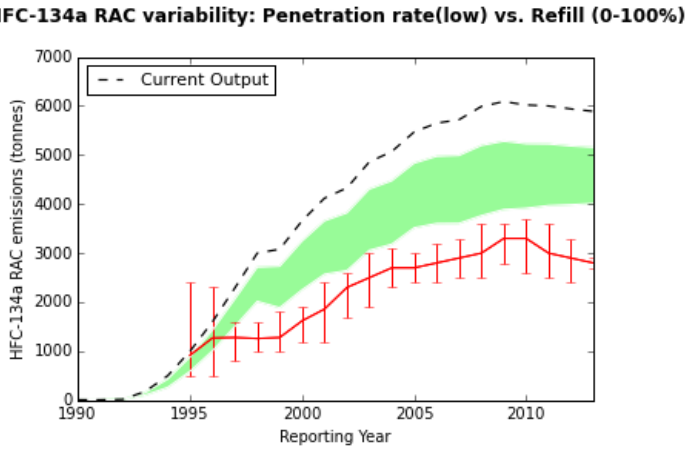

Figure 25: Combined theoretical variability introduced by combination of lowered penetration rate and refill input parameter. The dashed line indicates the reported output, and the solid red line indicates the independent top-down emissions estimates with respective error bars.

In Figure 25, lowering the penetration rate is shown, as expected, to reduce potential emissions of HFC-134a from the LMAC sector. This reduction is a direct response to fewer MAC units within the model; fewer units result in fewer sources of emission. While assuming a refill rate of 100% (all units refilled annually), the emission estimates remain significantly higher than top-down predictions. In 2010, this disagreement exceeds 1.3 Gg. A small level of agreement is observed when the refill parameter is reduce to 0% (refill of units does not occur). Agreement between top-down and inventory estimates (inventory estimates within top-down error bars) occurs between 1995 and 1997, after which the discrepancy remains low; in 2010, 0.2 Gg separates the theoretical inventory and top-down error bar limit.

After 2010, there is a notable divergence between estimates. While a plateau type effect is observed from the inventory, top-down annual figures begin to decrease. This separation suggests a slowing of emissions after 2010, perhaps as a result of new or improving technology, of which ICF International may not have been made aware. However, this cannot be confirmed, and may be as a result of unforeseen influences (i.e. noticeably fewer traffic collisions).

A third input with the potential to influence estimates are the refrigerant proportions, i.e. the ratio of all contributing coolants to the MAC sector, expressed as a percentage. In the original ICF International report, proportion assumptions are based on combined independent research and knowledge from industry experts. The percentage input values reflect the changing nature of MAC coolants, from first generation CFCs (CFC-12) to fourth generation HFOs (HFO-1234yf), in parallel with the demands of the Montreal Protocol and subsequent amendments.

To explore this hypothesis, the proportion of the market filled by HFC-134a was modified, and combined with varying refill rates to determine the likely impact. As a plausible scenario, a one year ‘market delay’ was introduced to the model; the ‘uptake’ of HFC-134a as the dominant coolant was offset by a year to determine any increased correlation with top down estimates.

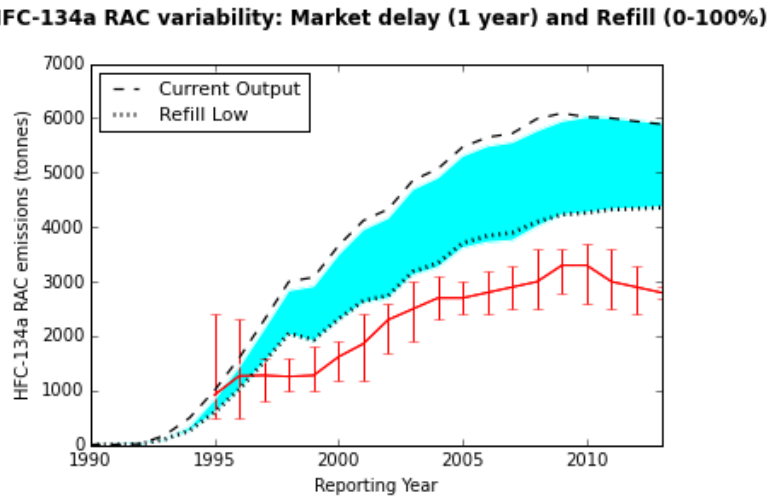

Figure 26: Combined theoretical variability introduced by combination of refill input parameter and one year delay of HFC-134a market proportion (%). The dashed line indicates the reported output and the dotted line indicates the lowest estimate generated by varying refill values (Figure 23).

As seen in Figure 26, a one-year market delay offers little in terms of theoretical estimate reduction. Compared to the current inventory, a small (approx. 0.05 Gg) reduction is observed throughout much of the time series, upon application of the delay. The reduction is lost after 2009, most likely as a result of the delayed introduction of low GWP (Global-Warming Potential) alternatives to HFC-134a. In the lower emissions scenarios, the hypothetical market delay offers no estimate reduction; in fact, when refill is set to 0%, emissions are marginally higher with introduction of the delay.

9.2.1 A '60% comparison'

In order to compare a revised refill parameter against other theoretical modifications to the RAC model, a standard refill value was chosen in order to reflect plausible trends in MAC refill. While a refill rate of 100% is considered excessive, clearly to assume a rate of 0%, where no unit refill occurs, is equally improbable. As a starting point, a refill value of 60% has been chosen, meaning 6 in 10 cars are refilled on an annual basis. The rest are not refilled during their lifetime. Further market research is required to determine a more accurate input value. To fully reflect refill trends, it is likely that a time-varying refill parameter is required; this may be considered in future work.

Figure 27 compares four theoretical scenarios against the actual inventory figures: 60% refill; 60% refill and minimum LMAC lifetime (11 years); 60% refill; one year HFC-134a market delay; 60% refill and minimum penetration rates;

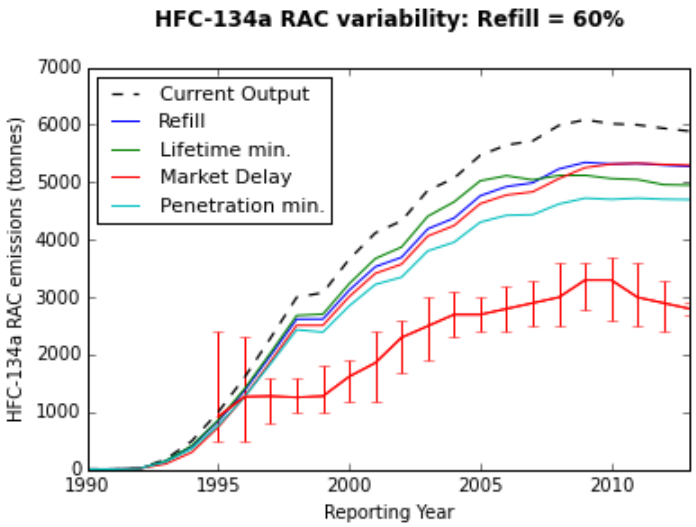

Figure 27: A comparison of parameter sensitivities against a set refill rate of 60%. The dashed black line indicates current inventory estimates, and the solid red line with error bars represents the independent top-down HFC-134a annual estimates.

Introducing a standard 60% refill rate offers significant theoretical reductions to inventory estimates however, a large discrepancy still exists when compared to top-down figures. All revised trends plateau post 2009, in disagreement with top-down estimates which show a downward trend. The greatest emissions reduction is observed upon the introduction of minimum penetration rates (1 and 60%, 1990 and 2008 respectively), with an approximate decrease of 1.3 Gg in 2010. Other scenarios are dominated by the reduction introduced by the refill modification; in particular, the market delay offers little change from the original 60% refill trend. Reducing the lifetime of LMAC units from 15 to 11 years gives a small reduction (approximately 0.3 Gg) after 2008. This arises as a result of limiting cumulative historic emissions: annual emissions are a sum of emissions from the unit lifetime.

In conclusion, while it can be said with reasonable confidence that the RAC refill parameter has a dramatic effect on emission estimates, it can only be considered a contributing factor for the discrepancy shown to exist between inventory and top-down estimates. Even at the extremities of parameter ranges, the disagreement between methods exceeds 1 Gg in most years after 1996. In order to pinpoint the source of this discrepancy, other input streams must be investigated. This study suggests two further work channels:

- Investigating further the RAC LMAC activity data. Changes in growth rate/total number of UK automobiles could influence annual emissions estimates.
- Apply the analysis techniques used here to investigate the calculation of emissions from the Aerosols sector. Original research highlighted large differences between UK aerosol emission factors and those of other European Nations. Given aerosol emissions represent around a third of the UK total for HFC-134a, such differences could account for a notable percentage of the over-reported totals.

This study has also highlighted the many advantages of Python as a modelling tool. Perhaps most importantly, the relative time savings that can be made when compared to spreadsheet processing times, and the importance of this saving when testing a wide range of output scenarios.

10 Recent Publications

Arnold, T., Ivy, D. J., Harth, C. M., Vollmer, M. K., Mühle, J., Salameh, P. K., Paul Steele, L., Krummel, P. B., Wang, R. H. J., **Young, D**., Lunder, C. R., Hermansen, O., Rhee, T. S., Kim, J., Reimann, S., **O'Doherty, S.,** Fraser, P. J., Simmonds, P. G., Prinn, R. G. and Weiss, R. F.: HFC-43-10mee atmospheric abundances and global emission estimates, Geophys. Res. Lett., 41(6), 2228–2235, doi:10.1002/2013GL059143, 2014.

Bergamaschi, P., Corazza, M., Karstens, U., Athanassiadou, M., Thompson, R. L., Pison, I., **Manning, A. J**., Bousquet, P., Segers, A., Vermeulen, A. T., Janssens-Maenhout, G., Schmidt, M., Ramonet, M., Meinhardt, F., Aalto, T., Haszpra, L., Moncrieff, J., Popa, M. E., Lowry, D., Steinbacher, M., Jordan, A., **O'Doherty, S**., Piacentino, S., and Dlugokencky, E.: Top-down estimates of European CH4 and N2O emissions based on four different inverse models, Atmos. Chem. Phys., 15, 715-736, doi:10.5194/acp-15-715-2015, 2015.

Fraser, P.J., B.L., Dunse, **A.J., Manning**, S. Walsh, R. H. J., Wang, P.B., Krummel, L. P., Steele, L.W., Porter, C. Allison, **O'Doherty**, **S**., **P.G., Simmonds**, J. Mühle, R.F. Weiss and R.G. Prinn, Australian carbon tetrachloride (CCl4) emissions in a global context, Environ. Chem., 11, 77, http://dx.doi.org/10.1071/EN13171, 2014.

Fraser, P. J., P. B. Krummel, L. P. Steele, C. Trudinger, D. M. Etheridge, N. Derek, **S. O'Doherty**, **P. G. Simmonds**, B. R. Miller, J. Mühle, R. F. Weiss, D. E. Oram, R. G. Prinn & R. H. J. Wang, Equivalent Effective Stratospheric Chlorine from Cape Grim Air Archive, Antarctic firn and AGAGE global measurements of ozone depleting substances, Baseline Atmospheric Program (Australia) 2009-2010, N. Derek P. B. Krummel & S. Cleland (eds.), Australian Bureau of Meteorology and CSIRO Marine and Atmospheric Research, Melbourne, Australia, 17-23, 2014.

Ganesan, A. L., Rigby, M., Zammit-Mangion, A., **Manning, A. J**., Prinn, R. G., Fraser, P. J., Harth, C. M., Kim, K.-R., Krummel, P. B., Li, S., Mühle, J., **O'Doherty, S. J**., Park, S., Salameh, P. K., Steele, L. P., and Weiss, R. F.: Characterization of uncertainties in atmospheric trace gas inversions using hierarchical Bayesian methods, Atmos. Chem. Phys., 14, 3855-3864, doi:10.5194/acp-14-3855-2014, 2014.

Ganesan, **A. L.**, **A. J. Manning**, A. Grant, **D. Young**, D. E. Oram, W. T. Sturges, J. B. Moncrieff, and **S. O'Doherty**, Quantifying methane and nitrous oxide emissions from the UK using a dense monitoring network. Atmos. Chem. Phys. Discuss., 15, 857-886, 2015.

Graziosi, F., Arduini, J., Furlani, F., Giostra, U., Kuijpers, L.J.M., Montzka, S.A., Miller, B.R**., O'Doherty, S.J**., Stohl, A., Bonasoni, P., Maione, M., European emissions of HCFC-22 based on eleven years of high frequency atmospheric measurements and a Bayesian inversion method, Atmospheric Environment (2015), doi: 10.1016/j.atmosenv.2015.04.042.

Hall, B. D., Engel, A., Mühle, J., Elkins, J. W., Artuso, F., Atlas, E., Aydin, M., Blake, D., Brunke, E.-G., Chiavarini, S., Fraser, P. J., Happell, J., Krummel, P. B., Levin, I., Loewenstein, M., Maione, M., Montzka, S. A., **O'Doherty, S**., Reimann, S., Rhoderick, G., Saltzman, E. S., Scheel, H. E., Steele, L. P., Vollmer, M. K., Weiss, R. F., Worthy, D., and Yokouchi, Y.: Results from the International Halocarbons in Air Comparison Experiment (IHALACE), Atmos. Meas. Tech., 7, 469-490, doi:10.5194/amt-7-469-2014, 2014.

Hossaini, R., M. P. Chipperfield, A. Saiz-Lopez, J. J. Harrison, R. von Glasow, R. Sommariva, E. Atlas, M. Navarro, S. A. Montzka, W. Feng, S. Dhomse, C. Harth, J. Mühle, C. Lunder, **S. O'Doherty**, **D. Young**, S. Reimann, M. K. Vollmer, P. B. Krummel, and P. F. Bernath, Growth in stratospheric chlorine from short-lived chemicals not controlled by the Montreal Protocol, Geophysical Research Letters, 2015GL063783, doi:10.1002/2015GL063783, 2015.

Khan, M. A. H., M. C. Cooke, S. R. Utembe, A. T. Archibald, P. Maxwell, W. C. Morris, P. Xiao, R. G. Derwent, M. E. Jenkin, C. J. Percival, R. C. Walsh, **T. D. S. Young**, **P. G. Simmonds**, G.

Nickless, **S. O'Doherty**, and D. E. Shallcross, A study of global atmospheric budget and distribution of acetone using global atmospheric model STOCHEM-CRI, Atmospheric Environment, 112, 269–277, doi:10.1016/j.atmosenv.2015.04.056, 2015.

Lunt, M. F., Rigby, M., Ganesan, A. L., **Manning, A. J**., Prinn, R. G., **O'Doherty, S**., Mühle, J., Harth, C. M., Salameh, P. K., Arnold, T., Weiss, R. F., Saito, T., Yokouchi, Y., Krummel, P. B., Steele, L. P., Fraser, P. J., Li, S., Park, S., Reimann, S., Vollmer, M. K., Lunder, C., Hermansen, O., Schmidbauer, N., Maione, M., Arduini, J., **Young, D**. and **Simmonds, P. G**.: Reconciling reported and unreported HFC emissions with atmospheric observations, Proc. Natl. Acad. Sci., 201420247, doi:10.1073/pnas.1420247112, 2015.

Maione, M., Graziosi, F., Arduini, J., Furlani, F., Giostra, U., Blake, D. R., Bonasoni, P., Fang, X., Montzka, S. A., **O'Doherty, S. J**., Reimann, S., Stohl, A., and Vollmer, M. K.: Estimates of European emissions of methyl chloroform using a Bayesian inversion method, Atmos. Chem. Phys., 14, 9755-9770, doi:10.5194/acpd-14-9755-2014, 2014.

O'Doherty, S., Rigby, M., Mühle, J., Ivy, D. J., Miller, B. R., **Young, D**., **Simmonds, P. G**., Reimann, S., Vollmer, M. K., Krummel, P. B., Fraser, P. J., Steele, L. P., Dunse, B., Salameh, P. K., Harth, C. M., Arnold, T., Weiss, R. F., Kim, J., Park, S., Li, S., Lunder, C., Hermansen, O., Schmidbauer, N., Zhou, L. X., Yao, B., Wang, R. H. J., Manning, A., and Prinn, R. G.: Global emissions of HFC-143a (CH3CF3) and HFC-32 (CH2F2) from in situ and air archive atmospheric observations, Atmos. Chem. Phys. Discuss., 14, 6471-6500, doi:10.5194/acpd-14-6471-2014, 2014.

S. J. **O'Shea**, G. Allen, M. W. Gallagher, K. Bower, S. M. Illingworth, J. B. A. Muller, B. T. Jones, C. J. Percival, S. J-B. Bauguitte, M. Cain, N. Warwick, A. Quiquet, U. Skiba, J. Drewer, K. Dinsmore, E. G. Nisbet, D. Lowry, R. E. Fisher, J. L. France, M. Aurela, A. Lohila, G. Hayman, C. George, D. B. Clark, **A. J. Manning**, A. D. Friend, and J. Pyle, Methane and carbon dioxide fluxes and their regional scalability for the European Arctic wetlands during the MAMM project in summer 2012, Atmos. Chem. Phys., 14, 13159-13174, 2014.

Patra, P. K., Krol, M. C., Montzka, S. A., **Arnold, T**., Atlas, E. L., Lintner, B. R., Stephens, B. B., Xiang, B., Elkins, J. W., Fraser, P. J., Ghosh, A., Hintsa, E. J., Hurst, D. F., Ishijima, K., Krummel, P. B., Miller, B. R., Miyazaki, K., Moore, F. L., Muhle, J., **O'Doherty, S**., Prinn, R. G., Steele, L. P., Takigawa, M., Wang, H. J., Weiss, R. F., Wofsy, S. C. and **Young, D**.: Observational evidence for interhemispheric hydroxyl-radical parity, Nature, 513(7517), 219–223 [online] Available from: http://dx.doi.org/10.1038/nature13721, 2014.

Rigby, M., Ronald G Prinn , **Simon O'Doherty** , Ben R Miller , Diane J Ivy , Jens Muhle , Chris M Harth , Peter K Salameh , **Tim Arnold**, Ray F. Weiss , Paul B Krummel , L Paul Steele , Paul J Fraser , **Dickon Young** , **Peter G Simmonds**, Recent and future trends in synthetic greenhouse gas radiative forcing, Geophys. Res. Lett., 41, doi:10.1002/2013GL059099, 2014.

Simmonds, P. G., **R. G. Derwent, A. J. Manning, A**. McCulloch, and **S. O'Doherty**: USA emissions estimates of CH_3CHF_2, CH_2FCF_3, CH_3CF_3, and CH_2F_2 based on in situ observations at Mace Head, Atmos. Env., 104, 27-38, doi:10.1016/j.atmosenv.2015.01/010, 2015.

Saikawa, E., Prinn, R. G., Dlugokencky, E., Ishijima, K., Dutton, G. S., Hall, B. D., Langenfelds, R., Tohjima, Y., Machida, T., Manizza, M., Rigby, M., **O'Doherty, S**., Patra, P. K., Harth, C. M., Weiss, R. F., Krummel, P. B., van der Schoot, M., Fraser, P. J., Steele, L. P., Aoki, S., Nakazawa, T., and Elkins, J. W.: Global and regional emissions estimates for N_2O, Atmos. Chem. Phys., 14, 4617-4641, doi:10.5194/acp-14-4617-2014, 2014.

Thompson, R. L., A. Stohl, L. X. Zhou, E. Dlugokencky, Y. Fukuyama, Y. Tohjima, S.-Y. Kim, H. Lee, E. G. Nisbet, R. E. Fisher, D. Lowry, R. F. Weiss, R. G. Prinn, **S. O'Doherty**, **D. Young**, and J. W. C. White, Methane emissions in East Asia for 2000–2011 estimated using an atmospheric Bayesian inversion, Journal of Geophysical Research: Atmospheres, 120(9), 2014JD022394, doi:10.1002/2014JD022394, 2015.

Thompson, R. L., Chevallier, F., Crotwell, A. M., Dutton, G., Langenfelds, R. L., Prinn, R. G., Weiss, R. F., Tohjima, Y., Nakazawa, T., Krummel, P. B., Steele, L. P., Fraser, P., **O'Doherty, S**., Ishijima, K., and Aoki, S.: Nitrous oxide emissions 1999 to 2009 from a global atmospheric inversion, Atmos. Chem. Phys., 14, 1801-1817, doi:10.5194/acp-14-1801-2014, 2014.

Thompson, R. L., Patra, P. K., Ishijima, K., Saikawa, E., Corazza, M., Karstens, U., Wilson, C., Bergamaschi, P., Dlugokencky, E., Sweeney, C., Prinn, R. G., Weiss, R. F., **O'Doherty, S**., Fraser, P. J., Steele, L. P., Krummel, P. B., Saunois, M., Chipperfield, M., and Bousquet, P.: TransCom N2O model inter-comparison – Part 1: Assessing the influence of transport and surface fluxes on tropospheric N2O variability, Atmos. Chem. Phys., 14, 4349-4368, doi:10.5194/acp-14-4349-2014, 2014.

Thompson, R. L., Ishijima, K., Saikawa, E., Corazza, M., Karstens, U., Patra, P. K., Bergamaschi, P., Chevallier, F., Dlugokencky, E., Prinn, R. G., Weiss, R. F., **O'Doherty, S**., Fraser, P. J., Steele, L. P., Krummel, P. B., Vermeulen, A., Tohjima, Y., Jordan, A., Haszpra, L., Steinbacher, M., **Van der Laan, S**., Aalto, T., Meinhardt, F., Popa, M. E., Moncrieff, J., and Bousquet, P.: TransCom N_2O model inter-comparison – Part 2: Atmospheric inversion estimates of N_2O emissions, Atmos. Chem. Phys., 14, 6177-6194, doi:10.5194/acp-14-6177-2014, 2014.

Vardag, S. N., Hammer, S., **O'Doherty, S**., Spain, T. G., Wastine, B., Jordan, A., and Levin, I.: Comparisons of continuous atmospheric CH4, CO2 and N2O measurements – results of InGOS travelling instrument campaign at Mace Head, Atmos. Chem. Phys., 14, 8403-8418, doi:10.5194/acp-14-8403-2014, 2014.

Weigelt, A., R. Ebinghaus, **A.J. Manning, R.G. Derwent, P.G. Simmonds, G.T. Spain**, S.G. Jennings, F. Slemr, Analysis and interpretation of 18 years of mercury observations since 1996 at Mace Head. Atmospheric Environment, Sept 2014.